Three-dimensional Sonoembryology

[1]Guillermo Azumendi, [2]Asim Kurjak

[1]Clinica Ecografia Centro Gutenberg, Malaga, Spain
[2]Medical School University of Zagreb, Sveti Duh Hospital, Zagreb, Croatia

Abstract: Three-dimensional ultrasound is advantageous in studying normal embryonic and fetal development, as well as providing information for families at risk for specific congenital anomalies by confirming normality. The introduction of high-frequency transvaginal transducers has resulted in remarkable progress in ultrasonographic visualization of early embryos and fetuses. Three-dimensional ultrasound imaging *in vivo* compliments pathologic and histologic evaluation of the developing embryo, giving rise to a new term: 3D sono-embryology.

Key word: Sonoembryology/Three-dimensional ultrasound/ Color Doppler/Power Doppler.

INTRODUCTION

Three-dimensional (3D) sonography has obtained important benefits among professionals interested in prenatal diagnostics. Although existing from the beginning in the early 1980s,[1,2] 3D sonography has become fully established in the last few years. This is mostly due to the exceptional development of computer processor technology essential for 3D imaging systems.

The main advantages of this new technology in obstetrics include improved assessment of complex anatomic structures, surface scan-analysis of minor defects, volumetric measurements of organs, spatial presentation of blood flow information and 3D examination of fetal skeleton.[3-8] Modern 3D systems are capable of generating surface and transparent views depicting the sculpture-like reconstruction of fetal surface structures or the X-ray-like images of fetal skeletal anatomy. Operating in planar mode, 3D orientation of tomograms is unlimited, despite limited probe manipulation or inadequate position of fetal structures. These imaging capabilities are extremely important during the first trimester of pregnancy when manipulation of the vaginal probe is restricted and obtainable ultrasound sections limited.[9] Additional progress is achieved owing to the permanent possibility of repeated analysis of previously saved 3D volumes and elimination of surrounding structures.[1,10] It should be emphasized that in the field of prenatal diagnosis the 3D technique is complementary to the conventional two-dimensional (2D) technique, rather than offering an alternative.[11] However, 3D imaging is superior in specific diagnostic problems. A comparison of 2D and 3D techniques shows that 3D provides a diagnostic gain in a large percentage of cases. This is due to the possibility of surface and transparent mode imaging that makes accurate topographic depiction of the desired image plane much easier.[1,12,13]

A detailed sonogram of the fetus during the first trimester can be obtained due to the large amount of amniotic fluid. Moreover, 3D sonography absolutely superior to the standard 2D sonography in assessment during the first trimester of pregnancy. 3D sonography tremendously reduces the time of exposure of embryo to the ultrasound beam. Volume acquisition takes only a few seconds. Image processing and analysis is done off-line, without any time limitations. Sonographers can choose between two principal modes of imaging: the planar mode and the full 3D image. In the planar mode the object is simultaneously projected onto three perpendicular planes (Fig. 1). There is no limit in object rotation or in the number of tomograms of different sections of the analyzed object. Planar mode enables superb precision of measurement. Full 3D mode is particularly useful in presenting the 3D interrelationship of

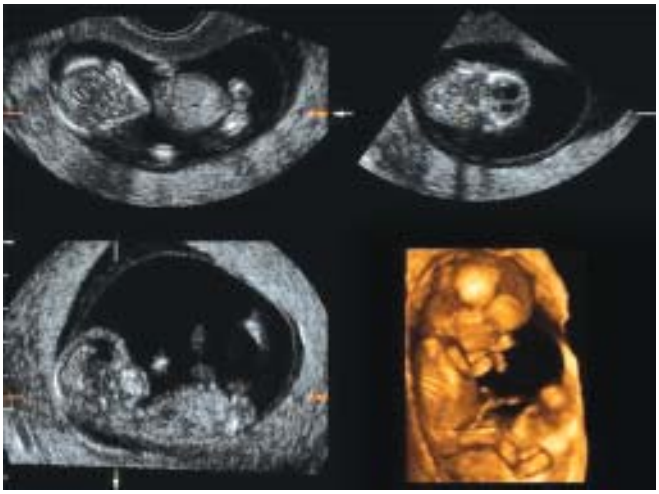

Fig. 1: Three section planes of 3D ultrasound. These three planes (frontal, transverse, mid-sagittal) are perpendicular to one another at the three axial center of rotation

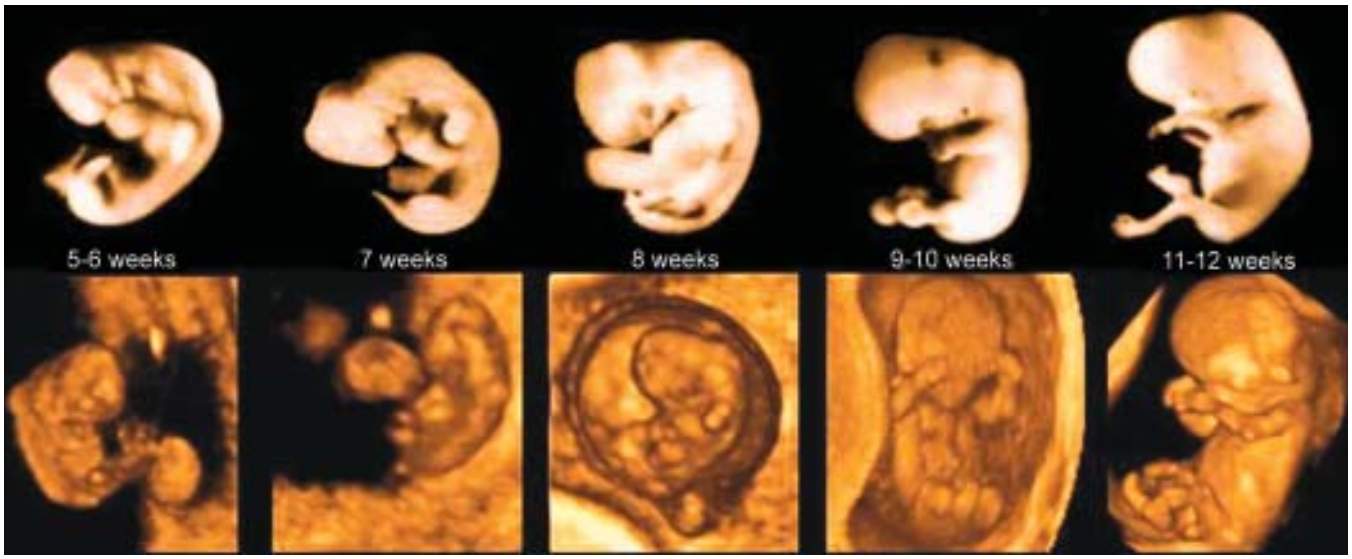

Fig. 2: Comparison betwen computer animation model of embrional development and a series of *in vivo* obtained images of the human embryo by 3D sonography, emphasizing development of the embryo in the early pregnancy

different organs or the skeleton. Sonographers can change between different modalities of image rendering, emphasizing the outer surface or presenting inner structures through the transparent mode.

3D sonography can improve accuracy and success rate of nuchal translucency measurement in pregnancy between 10 and 14 weeks' gestation. In a series of 120 pregnancies Kurjak and Kupesic[14] were able to obtain the mid-sagittal section and measure nuchal translucency in 100% of cases using 3D transvaginal sonography. Using standard 2D sonography this was possible in only 85% of cases. Due to the superb quality of images, 3D sonography enables detection of developmental anomalies.[15-21] 3D sonography will certainly improve early detection of fetal anomalies, and possibly become the screening method for them. In addition, 3D sonography produced better intra-observer reproducibility of results. 3D sonography with its potential for complex and sophisticated post processing of images has proved to be a useful tool in experimental embryology. Using a special off-line imaging computer device Blaas et al[22] produced a series of *ex vivo* obtained images of the human embryo, emphasizing development of the brain cavities during the first trimester. This new technology has moved embryology from postmortem studies to *in vivo* environment (Fig. 2).

Developments on the ultrasound technology enabled us to expand investigations of early placental vascular supply. 3D power Doppler is a unique instrument that enables assessment of vascular signals within the whole investigated area. Hemodynamical changes included in the process of early placentation are one of the most exciting topics in investigation of early human development. This investigation was designed as an observational cross-sectional study. After acquirement of the volume containing 3D power Doppler data of the pregnant uterus, the signals belonging to the chorion were isolated. Vascular 3D measurements were undertaken through 3D power histogram and expressed by Vascularization Index (VI) and Vascularization Flow Index (VFI). Volume of the chorion increased exponentially throughout the observation period. The VI and VFI positively correlated with the crown-rump length and chorion volume (Fig. 3), and showed gradual increment through the investigation period. This investigation produced results confirming gradual augmentation of the loci and intensity

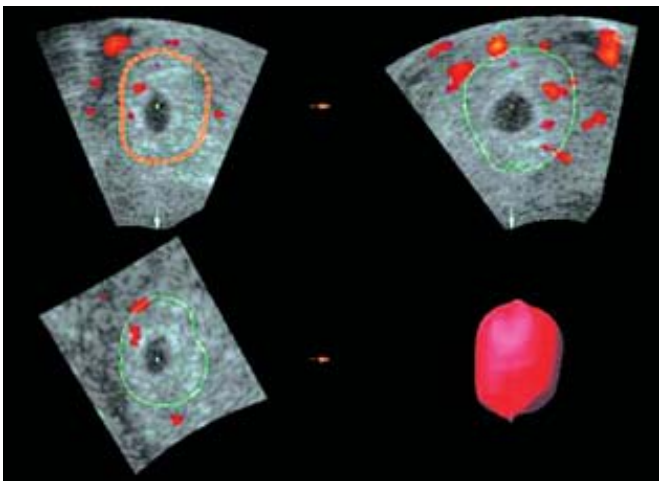

Fig. 3: Volume calculation (VOCAL) software feature enables measurement of chorionic volume from the surrounding structures and quantitative measurement of vascular signals

of the intervillous flow in pregnancies between five and eleven gestational weeks.[23,24]

3D ULTRASOUND FINDINGS FROM OVULATION TO IMPLANTATION

Uterus

It is understood that normal early human development determined by uterine perfusion, implantation process and chromosomal structure of the fetus. Insufficient implantation and inadequate uterine blood flow can be non-invasively perceived by Doppler technique. Consequently, entire set of new undiscovered circumstances concerning this matter is accessible for research.

After ovulation, there is a brief interval throughout which endometrial receptivity is at its maximum. During these few days, a blastocyst traveling to the uterine cavity can achieve a physical contact with the endothelial lining and eventually-implant. At the beginning of its attachment, the blastocyst is directed with the inner cell mass toward the endometrium. Furthermore, the trophoblast produced action of the proteolysis enzymes which enabled penetration and erosion of the uterine mucosa. During implantation, the trophoblast erodes lying near maternal capillaries, and maternal blood enters to a direct contact with the conceptus. The intercommunicating lacunar network begins to be the intervillous space of the placenta (Fig. 4).

Throughout the 4th week the migrating trophoblast penetrates the uterine wall and invades venous sinusoids of increasing size and superficial arterioles. Trophoblastic cells can be discovered inside the spiral arteries at approximately the 6th week following fertilization. Increasing blood flow produces progressive distention of these arteries into the uteroplacental arteries having the ability of adapting the increasing blood supply.

Endometrium

With the advance of three-dimensional (3D) ultrasonography it became possible to perform reliable sonographic endometrial volume calculations and to correlate them with pregnancy rates undergoing *in vitro* fertilization (IVF).[15,16] More recently, subendometrial blood flow was quantitatively analyzed by using the color histogram mode in 3D power Doppler (Fig. 5).[25]

By 3D ultrasound, it is possible to us to determine the quantity of the endometrial volume and predict the probability of implantation because quantitative volume measurements appear to be more accurate than estimation of the endometrial thickness. It is suggested that quantification of endometrial volume by 3D ultrasound in combination with blood flow studies may be the most useful method to predict pregnancy rates as a sequel of the medically assisted reproduction.[25]

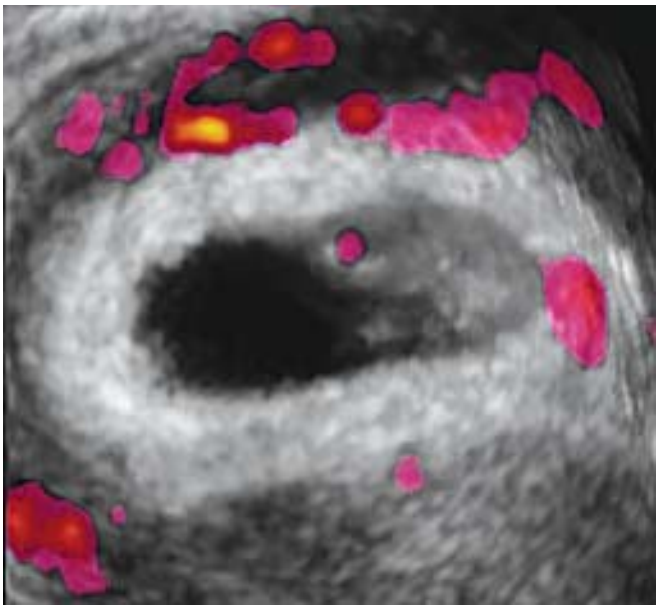

Fig. 4: 3D power Doppler showing uterine perfusion during implantation, the trophoblast erodes lying near maternal capillaries and maternal blood enters to a direct contact with the conceptus

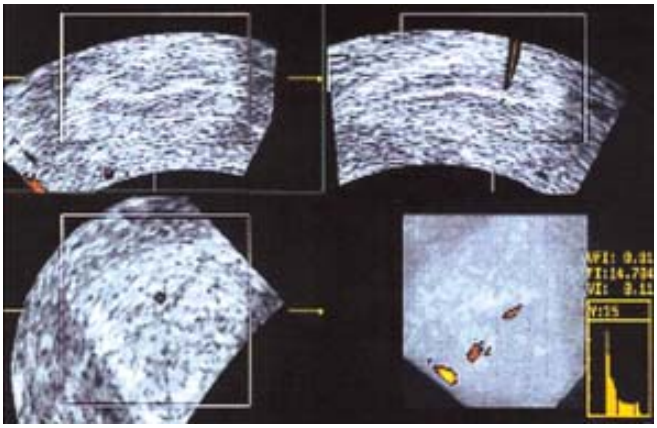

Fig. 5:. 3D power Doppler image of the endometrium on the day of embryo transfer. Note the color histogram at the bottom right, which shows vascularization flow index

Ovaries

At the 8th week of gestation, luteal flow becomes less detectable and the visualization rate is 60 to 80%. There is no obvious connection between the 2D ultrasonographic and Doppler characteristics of the corpus luteum and first trimester pregnancy outcome. The role of 3D ultrasound in the evaluation of the corpus luteum morphology and vascularity has still to be investigated.

Events Following Implantation

The earliest visible sign of pregnancy is a new formed gestational sac that can be seen during 5th week of pregnancy.

Fig. 6: 3D images of gestational sac during 5th week of pregnancy

Ultrasonographically, it is presented as a hypoechoic oval structure, surrounded by a hyperechoic ring, situated asymmetrically in the uterine cavity (Fig. 6). Gestational sac at this time measures approximately 5 mm and grows 1 to 2 mm per day.

As the fetal and placental structures develop, their vascular network becomes more pronounced. Hence, it is possible to observe three separate and yet unified units: the maternal, placental and fetal portions of the vascular network.

Maternal Portion

The maternal portion of the placental circulation consists of the main uterine arteries and their branches that spread throughout the uterus until they reach the decidual plate of placenta. The main uterine arteries originate from the internal iliac arteries, and they give off branches, which extend inward for about a third of the myometrium thickness without significant branching. At this point, they subdivide into an arcuate wreath encircling the uterus. From this network, smaller branches called the radial arteries, arise and are directed towards the uterine lumen. The radial arteries branch into basal arteries and endometrial spiral arteries as they pass the myometrial-endometrial border. Basal arteries, that are relatively short, terminate in a capillary bed that serves the stratum basale of the endometrium. The spiral arteries project further into the endometrium and terminate in a vast capillary network that serves the functional layer of the endometrium. All of them can be clearly identified in the pregnant uterus by their anatomical position and characteristic waveform profile.

Intrauterine placental development requires adaptive changes of the uterine vascular environment. The fact that the uterine vascular network elongates and dilates throughout the pregnancy is well known from anatomical studies.[26]

Doppler Findings

Flow velocity waveforms from small arteries show significantly lower pulsatility and blood velocity as compared to the main uterine artery. The branching of the uterine circulation and the increased total vascular cross-sectional area, which results in lower impedance to blood flow, is the background of this phenomenon. Most authors have demonstrated that the progressive decrement in the impedance to blood flow observed in the main uterine artery during early pregnancy occurs in all the segments of the uteroplacental circulation.[27-30]

Transvaginal color and pulsed Doppler allows identification of the uterine vascular transformation. Furthermore, the invasion of larger maternal blood vessels of higher pressure results in higher velocity and larger diastolic component of Doppler signal.

Kurjak and colleagues[31] have pointed to vascular changes in early pregnancy even before visualization of the gestational sac. With advancing gestational age, impedance to blood flow decreases from the main uterine to spiral arteries. At the same time, an increase in blood flow by means of peak-systolic velocity has a decreasing trend from the uterine, through the arcuate to the radial arteries. The increment in blood flow through the uterine network is probably caused by an urgent need of the placenta and fetus for nourishment.

Uterine Artery Blood Flow in Non-pregnant and Pregnant Patients

The main uterine artery can be visualized at the level of the internal cervical os, as it approaches the uterus laterally and curves upward alongside the uterine body. Pulsed Doppler waveform profiles of the main uterine artery are characteristic, comprising a high peak-systolic component with a characteristic notch in the protodiastolic part and very low end-diastolic flow. Numerous Doppler studies have demonstrated a gradual decrement in the uterine artery resistance index during the first trimester of pregnancy.[27-30]

Characteristic notch in the protodiastolic part of sonogram is gradually disappearing; diastolic flow is characterized by high velocity, and difference between systolic and diastolic flow velocities decreases. This kind of changes indicates normal development of pregnancy (trophoblast invasion). Obviously, this decrement continues during the second trimester of pregnancy and can be observed in all the segments of the uteroplacental circulation.

Arcuate and Radial Arteries Blood Flow in Non-pregnant and Pregnant Patients

Arcuate arteries may be seen within the outer third of the myometrium, while the radial arteries are identified within the two inner thirds of the myometrium. Doppler sonograms of the

arcuate and radial arteries are very similar, with moderate peak-systolic and diastolic components of blood flow. However, differences exist in the values of the resistance (RI) or pulsatility (PI) indices. These are lower in the radial than in the arcuate arteries, corresponding to the lower peripheral impedance to blood flow.

Normal Finding of Spiral Arteries in Pregnant Patients

During early pregnancy, the spiral arteries are progressively converted to nonmuscular dilated tortuous channels. The normal musculo-elastic wall is replaced with a mixture of fibrinoid material and fibrous tissue. Easy to be detected above the chorion (near the placental implantation site), spiral arteries are characterized by lower resistance index and higher peak systolic velocities followed by turbulent flow (Fig. 7). This kind of flow is typical for wide tortuous blood vessels and has hemodynamic characteristics of an arteriovenous shunt. The active trophoblast induces vascular adaptation, which ensures adequate blood supply to the growing embryo.

Pulsed Doppler waveform signals obtained from spiral arteries show low impedance to blood flow and a characteristic spiky outline. The sonogram presents the blood flow from more than one spiral artery. The spiral arteries change their wall structure with gestation and become vessels with completely different hemodynamics in relation to other arteries of the uteroplacental circulation.

PLACENTA

Development and the Ultrasound Imaging

Primary chorionic villi develop between 13th and 15th day after the ovulation (during 4th week of gestation) and mark the beginning of the placental development. At the same time, the formation of blood vessels starts in the extraembryonic mesoderm of the yolk sac, the connecting stalk and the chorion.[32] By 18 to 21 days (during 5th week of gestation), the villi have become branched and the mesenchymal cells within the villi have differentiated into blood capillaries and formed an arteriocapillary venous network. Chorionic villi cover the entire surface of the gestational sac until the end of the 8th week. At that time, the villi on the side of the chorion proliferate towards the decidua basalis to form the chorion frondosum, which develops into the definitive placenta. The villi in contact with the decidua capsularis begin to degenerate and form an avascular shell, known as the chorion laeve or smooth chorion. The placenta is mostly derived from fetal tissues, when maternal component contributes little to the architecture of the definitive placenta.

Normal placentation requires a progressive transformation of the spiral arteries and an infiltration of trophoblastic cells into the placental bed. These physiological changes normally

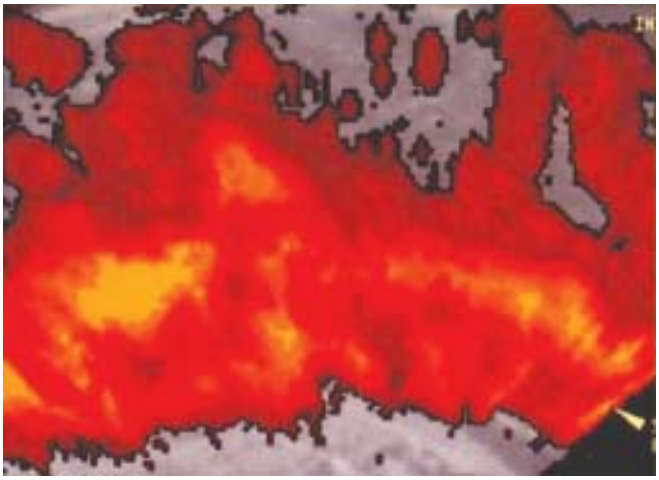

Fig. 7: Transvaginal 3D power Doppler image on early pregnancy demonstrate blood floow signal derived from spiral arteries

extend into the inner third of the myometrium, and in normal pregnancies, all the spiral arteries are transformed into uteroplacental arteries before 20 weeks of gestation.[33] In some cases of early pregnancy failure and pregnancy-induced hypertension, there is an adequate placentation with a defective transformation of spiral arteries.[34]

3D Power Doppler Studies in Assessment of Early Chorionic Circulation

New developments on the cutting edge of the ultrasound technology enabled us to expand investigations of early placental vascular supply. 3D power Doppler is able to depict the integral 3D image of placenta and embryo and their vascular network.[5,23] Additionally, it is possible to quantify and express numerically data related to vascular signals in the investigated volume.

Development of the process of placentation begins after the first contact between trophoblast and decidua has been established. There are two waves of trophoblastic invasion. First occurs at 8 weeks of pregnancy. It is characterized by invasion of interstitial trophoblast invasion into the myometrium and cytotrophoblast (endothelial trophoblast) into complete decidua, but not myometrium. Second wave is characterized just by invasion of endothelial trophoblast into the myometrium and occurs between 16 and 18 weeks of gestation.[35]

Uteroplacental arteries are not responsive to the autonomous nervous system. In the second lunar month, the intervillous space increases as the result of the extensive branching of the villi. The intervillous space, combined with the villi, is the functional unit of the human placenta, where maternal-fetal metabolic exchange occurs.[36] In this period, many terminal parts of the spiral arteries near the intervillous space contain plugs of cytotrophoblastic cells. At the same time, centrally placed communications between the decidual veins are numerous and

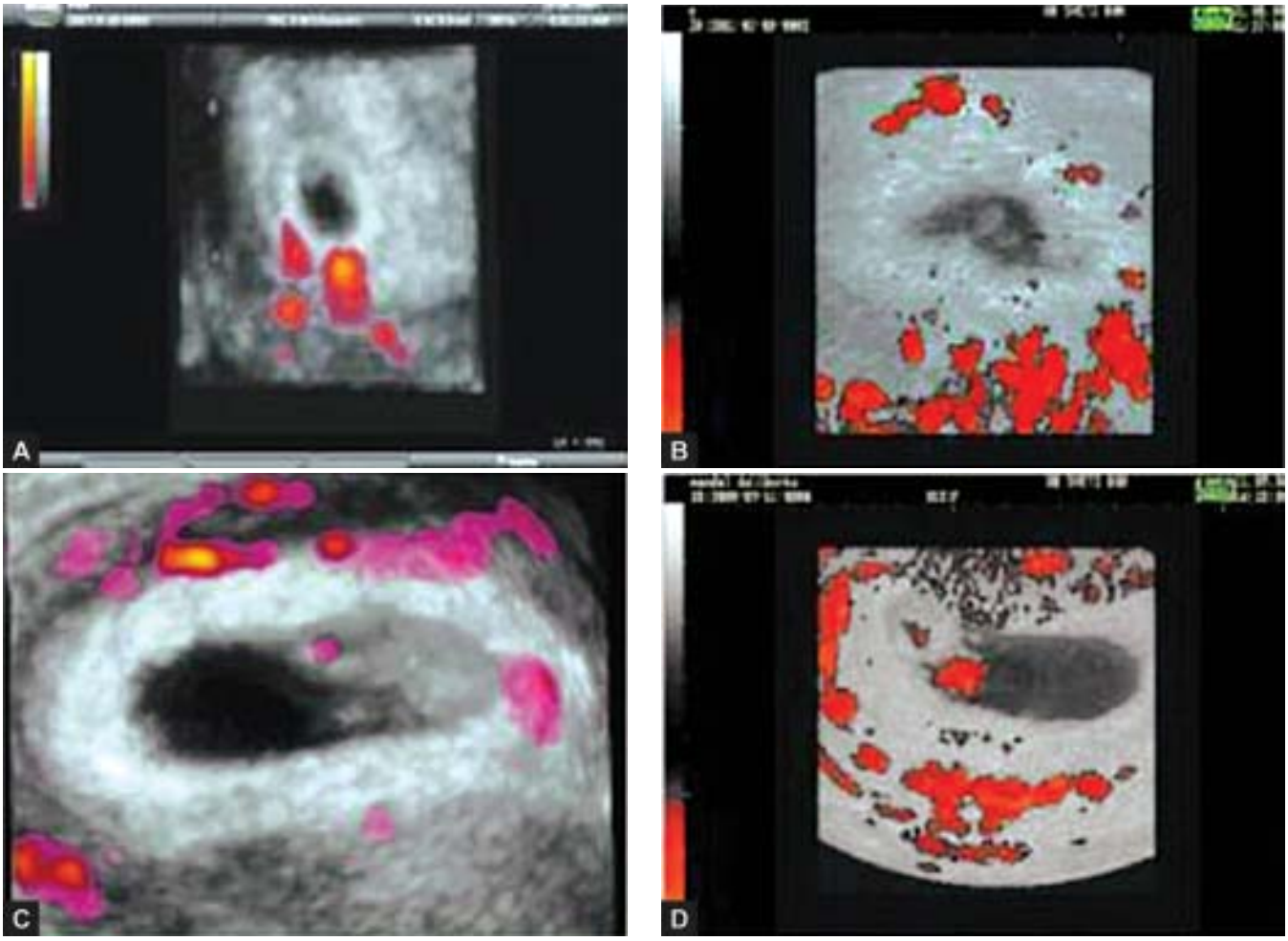

Figs 8A to D: 3D power Doppler image of early gestation and its vascular supply
(A) 5 weeks, (B) 6 weeks, (C) 8 weeks, (D) 9 weeks

large. After 40 days spiral arteries show direct openings into the intervillous space and the cytotrophoblastic cells appear within their lumen. The maternal blood reaches the intervillous space through the gaps between the cells of the endovascular trophoblast. These events can be nicely studied by 3D color and power Doppler ultrasound (Figs 8A to D).

During pulsed Doppler analysis two types of waveform can be visualized: pulsatile arterial-like, and continuous venous-like flow. Lumen of the spiral arteries is never completely obstructed by the trophoblastic plugs. These data indicate that establishment of the intervillous circulation is a continuous process rather than an abrupt event at the end of the first trimester. Kurjak et al[37] did cross-sectional study in a group of patients in gestational age 5 to 11 weeks. After acquirement of the volume containing 3D power Doppler data of the pregnant uterus, the signals belonging to the chorion were isolated. Vascular 3D measurements were undertaken and expressed by Vascularization Index (VI) and Vascularization Flow Index (VFI). Volume of the chorion increased exponentially throughout observation period. The VI and VFI positively correlated with the crown-rump length (CRL) and chorion volume, and showed gradual increment through the investigation period (Figs 9A to E).

FETAL PORTION

The assessment of the fetal portion of circulation includes the umbilical and fetal circulation. Hemodynamic changes in the umbilical artery represent the placental side of the uteroplacental circulation. Signals from the umbilical artery may be clearly visualized at the embryo's lateral edge connected to the placenta. The fetal circulation is usually analyzed through assessment of the fetal heart, fetal aorta, carotid arteries and intracranial circulation (middle cerebral artery in particular) (Fig. 10).

The appearance of blood flow in these arteries is described separately for each gestational week and compared to the main

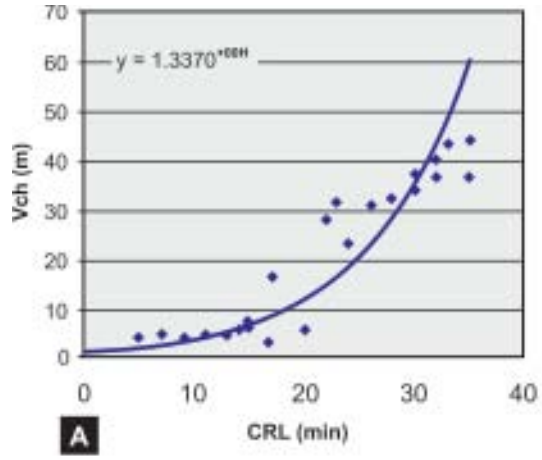

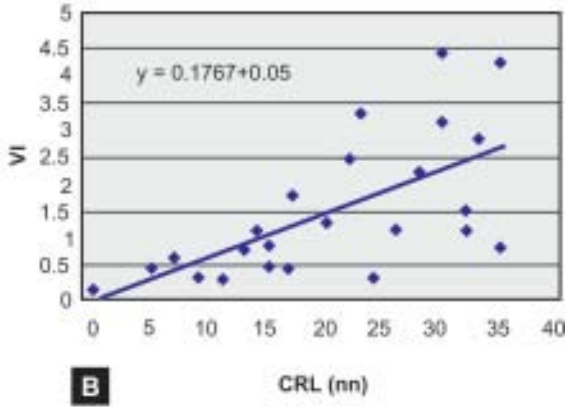

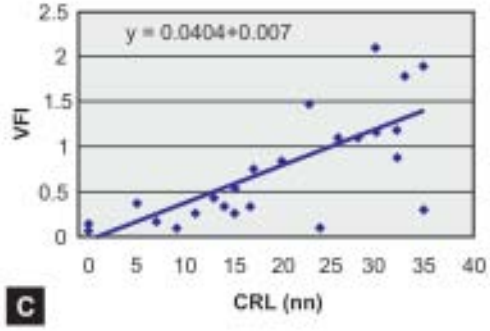

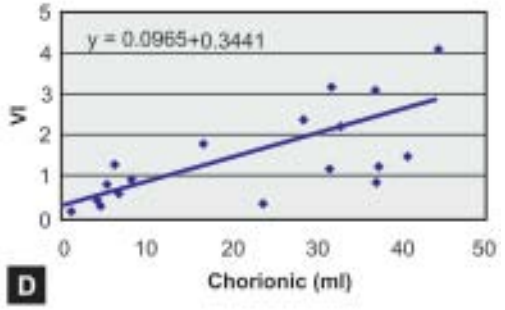

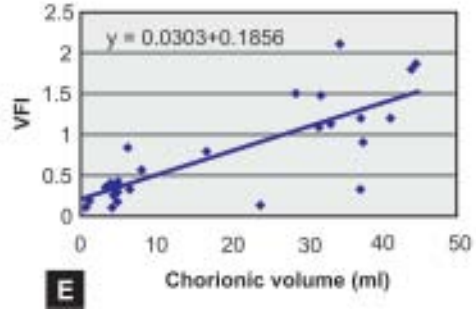

Figs 9A to E: Corelation between vascular activity in the chorion detected by 3D power Doppler: (A) Chorionic volume (Vch) related to the crown-rump length (CRL), (B) Chorionic vascularization index (VI) related to the crown-rump length (CRL), (C) Chorionic vascularization flow index (VFI) related to the crown-rump length (CRL), (D) Chorionic vascularization index (VI) related to the chorionic volume, (E) Chorionic vascularization flow index (VFI) related to the chorionic volume

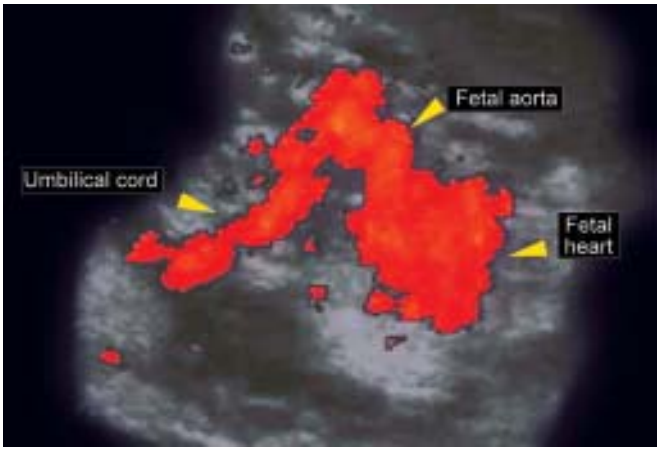

Fig. 10: 3D power Doppler demonstrated signals from the umbilical artery, fetal heart, fetal aorta at the embryo's lateral edge connected to the placenta

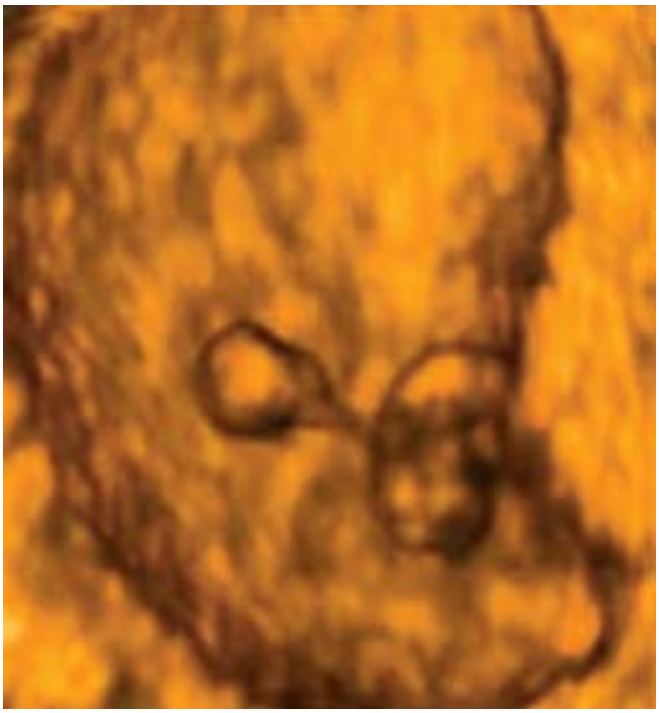

Fig. 11: 3D ultrasond in 5 weeks of pregnancy. The deep neural groove and the first somites are present. The embryo is almost straight and somites produce conspicuous surface elevation. Gestational sac can be visualized as a small spherical anechoic structure placed inside one of the endometrial leafs

histological and conventional gray-scale ultrasound findings. Kurjak and Kupesic[38] used combined B-mode and power Doppler imaging in order to evaluate fetal growth and development of fetal circulation. Different rendering modalities were used in color-coded data processing and presentation. A minimum-intensity projection of the vascular network was used to create a translucent image, and a maximum-intensity projection was applied for a surface rendered vascular image. The former was superior in assessment of the spatial inter-relationship of the vascular structures, and the latter was useful in the assessment of the morphology and outer surface of a confined vascular structure.

The 5th Week

Characteristic Embryological Findings

The deep neural groove and the first somites are present. The embryo is almost straight and somites produce conspicuous surface elevation. The heart prominence is distinct and the optic pits are present.

The attenuated tail with its somites is also a characteristic feature.

3D Ultrasound Findings

Gestational sac can be visualized as a small spherical anechoic structure placed inside one of the endometrial leafs. 3D sonography enables precise measurement of exponentially expanding gestational sac volume during the first trimester (Fig. 11). Kupesic and co-workers[39] found that 3D measurement of yolk sac volume and vascularity may be predictive of a pregnancy outcome. Using this non-invasive modality one can obtain multiplanar and surface images in reduced scanning time. Surface images seem to be beneficial in the evaluation of the yolk sac echogenicity and detection of the hyperechoic yolk sac which may indicate chromosomal abnormality. Automatic and manual volume calculation allows analysis of the precise relationship between the yolk sac and gestational sac volumes, as well as assessment of the correlation between yolk sac volume and CRL measurements. Planar mode tomograms are useful for detecting the embryonic pole inside the gestational sac. The embryo itself can be seen 24 to 48 hr after visualization of the yolk sac, at approximately 33 days after menstruation, at which is 2 to 3 mm long.[40] Adjacent to the yolk sac, embryo can be seen as a small straight line measuring by the end of 5th gestational week.

3D Power Doppler Findings

3D power Doppler reveals intensive vascular activity surrounding the chorionic shell staring from the first sonographic evidence of the developing pregnancy during the 5th week of gestation (Fig. 12). Gestational sac can be detected as a tiny ring shaped structure at the beginning of gestational age of five weeks. 3D power Doppler reveals intense vascular activity surrounding it. A hyperechoic chorionic ring is interrupted by color-coded sprouts of early intervillous and spiral artery blood flow. At the end of the fifth week, when the gestational sac

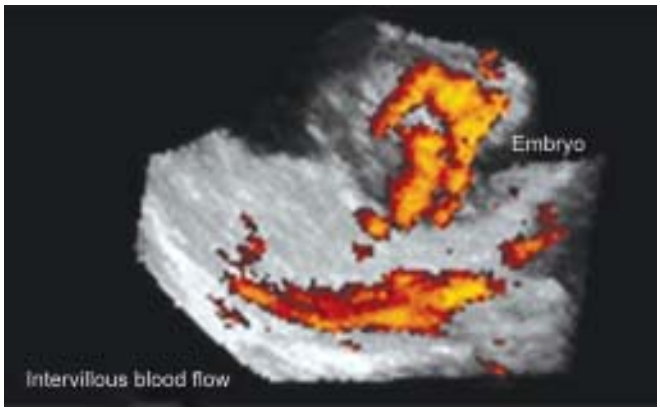

Fig. 12: 3D power Doppler reveals intensive vascular activity surrounding the chorionic shell staring from the first sonographic evidence of the developing pregnancy during the 5th week of gestation

exceeds 8 mm, the small secondary yolk sac is visible as the earliest sign of the developing embryo.

The 6th Week

Characteristic Embryological Findings

The embryo has a C-shaped curve. The growth of the head (caused by the rapid development of the brain) exceeds that of the other regions.

3D Ultrasound Findings

Rounded bulky head and thinner body characterize 3D image of an embryo during the 6th week of pregnancy (Fig. 13). The head is prominent due to the developing forebrain. Limb buds are rarely visible in this stage of pregnancy. However, umbilical cord and vitelline duct are always clearly seen. At 6 weeks of gestation ductus omphalomesentericus can be as much as three to four times the length of the embryo itself. The amniotic membrane is also visible, initially at the dorsal part of the embryo. A few days later it surrounds the embryo but not the yolk sac, which remains in the extracelomic cavity.

3D Power Doppler Findings

Aortic and umbilical blood flow is well depicted. Initial branches of the umbilical vessels are visible at the placental umbilical insertion (Fig. 14). 3D power Doppler detects embryonic heartbeats as early as five weeks and four days menstrual age, at the embryo CRL of 3 ± 4 mm. At this very early stage, this finding may help clinicians to diagnose the viability of the pregnancy. Near the end of the sixth week first signs of aortic and umbilical blood flow within the embryo's trunk are visible. The initial branches of the umbilical vessels are visible at the placental umbilical insertion.

Fig. 13: Rounded bulky head and thinner body characterize 3D image of an embryo during the 6th week of pregnancy. The head is prominent due to the developing forebrain. Limb buds are rarely visible in this stage of pregnancy

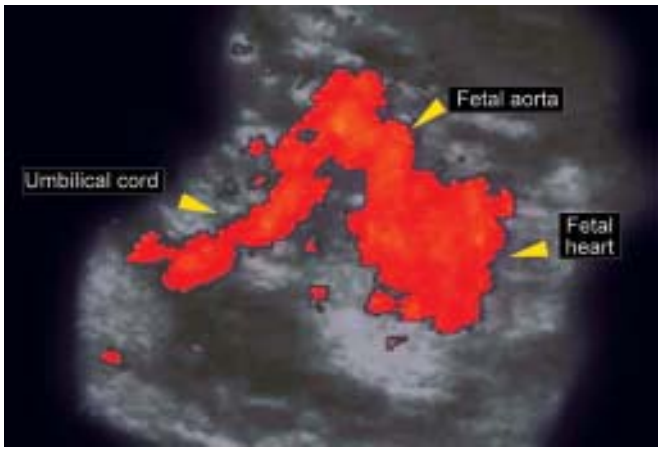

Fig. 14: 3D power Doppler image of an embryo during the 6th week of pregnancy. Aortic and umbilical blood flow is well depicted. Initial branches of the umbilical vessels are visible at the placental umbilical insertion

The 7th Week

Characteristic Embryological Findings

The head is now much larger in relation to the trunk and is more bent over the cardiac prominence. The trunk and neck have begun to straighten. Hand and foot plates are formed and digital or finger rays started to appear.

3D Ultrasound Findings

During the 7th gestational week spine gradually becomes visible, as well as limb buds, lateral to the body. Amnion can be seen as a spherical hyperechoic membrane, still close to the embryo. Chorion frondosum can be distinguished from the chorion laeve. Fast development of rhombencephalon (hindbrain) occurs. This process gives even more prominence to the head. Head becomes the dominant embryonic structure. Using the multiplanar mode, developing vesicles of the brain can be depicted as anechoic structures inside the head. The biggest, and usually the only visible, is rhombencephalon placed on the top of the head (vertex). The head is strongly flexed anterior being in contact with the chest (Fig. 15). The hypoechogenic brain cavities could be identified, including the separated cerebral hemispheres. The lateral ventricles are shaped like small round vesicles. The cavity of the diencephalon (future third ventricle) runs posterior. In the smallest embryos, the medial telencephalon forms a continuous cavity between the lateral ventricles. The future foramen of Monroe are wide. In the sagittal plane, the height of the cavity of the diencephalon (future third ventricle) is slightly greater than that of the mesencephalon. Thus, the wide border between the cavities of the diencephalon and the mesencephalon is indicated. The curved tubelike mesencephalic cavity (future Sylvian aqueduct) lies anterior, its rostral part pointing caudal. It straightens considerably during the following weeks.

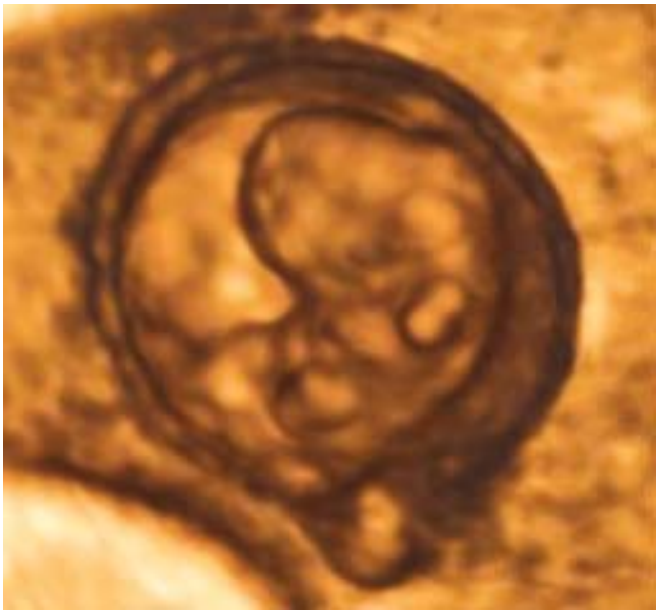

Fig. 15: 3D image during the 7th gestational week, spine gradually becomes visible, as well as limb buds, lateral to the body. Amnion can be seen as a spherical hyperechoic membrane, still close to the embryo

3D Power Doppler Findings

Besides the aorta and umbilical blood flow, at the end of the 7th week 3D power Doppler depicts features of early vascular anatomy on the base of the skull. Vessels are evolving laterally to the mesencephalon and cephalic flexure. Apart from embryonic circulation, 3D power Doppler can obtain blood flow signals from the intervillous space. The gestational sac occupies about one-third of the uterine volume. The main landmark now is an echogenic fetal pole consisting of embryo adjacent to a cystic yolk sac. The intracranial circulation becomes visible during the seventh week of gestation. At this time discrete pulsations of the internal carotid arteries are detectable at the base of the skull (Fig. 16).

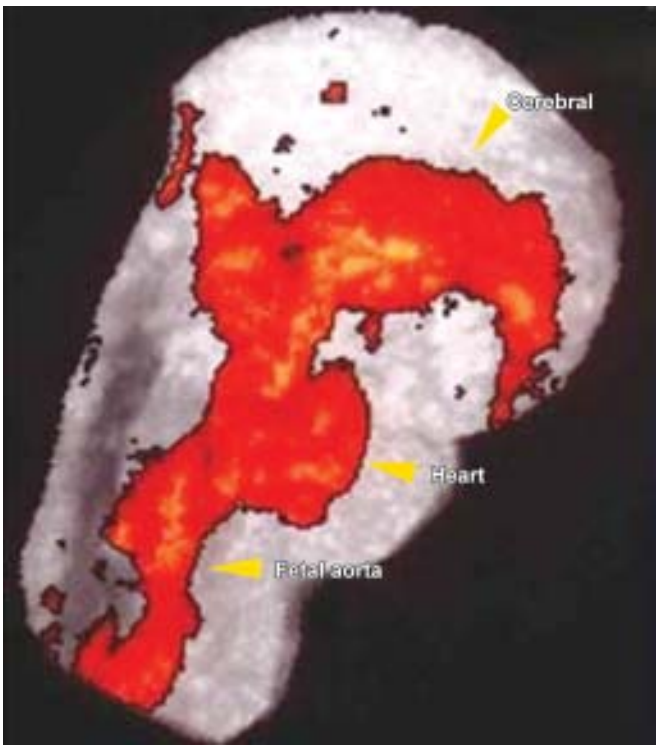

Fig. 16: 3D Power Doppler findings demonstrated the aorta and umbilical blood flow, at the end of the 7th weeks. 3D power Doppler depicts features of early vascular anatomy on the base of the skull. The intracranial circulation becomes visible during this gestational age

The 8th Week

Characteristic Embryological Findings

By the beginning of the 8th week, the embryo has developed a skeleton, which is mostly cartilaginous and gives form to its body. The communication between the primitive gut and the yolk sac has been reduced to a relatively small duct (the yolk stalk).

3D Ultrasound Findings

The most characteristic finding is a complete visualization of the limbs, which end in thicker areas that correspond to the future hands and feet. The shape of the face begins to appear but is not clearly seen (Fig. 17). The great majority of embryos

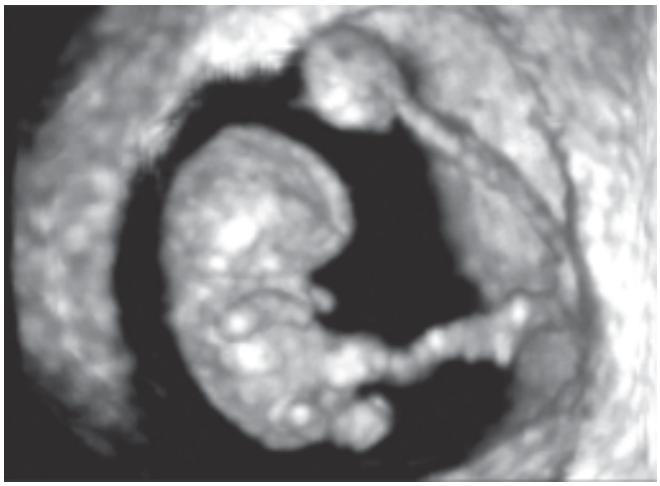

Fig. 17: 3D Ultrasound Findings demonstrated complete visualization of the limbs, which end in thicker areas that correspond to the future hands and feet. The shape of the face begins to appear but is not clearly seen. The communication between the primitive gut and the yolk sac has been reduced to a relatively small duct (the yolk stalk)

show a cranial pole flexion that makes it almost impossible to see the face. Insertion of the umbilical cord is visible on the anterior abdominal wall. During the 8th week of pregnancy there is expansion of the ventricular system of the brain (lateral, third and midbrain ventricles). Due to these processes the head erects from the anterior flexion. The vertex is now located over the position of the midbrain. Structures of the viscerocranium are not visible due to their small size. Arms and feet are clearly visible. Insertion of the umbilical cord is visible on the anterior abdominal wall. During the 8th and 9th week the developing intestine is being herniated into the proximal umbilical cord.

Blaas and co-workers[41] reported on a 7 weeks and 5 days gestational age embryo whose brain structures were analyzed in detail by 3D ultrasound. They described distinct hemispheres how the rhombencephalic cavity (future fourth ventricle) deepens gradually with the growth of the embryos, at the same time decreasing its length.[41] At this time, it has a pyramid-like shape with the central deepening of the pontine flexure as the peak of the pyramid.[42]

3D Power Doppler Findings

During the 8th and 9th week, developing intestine is being herniated into the proximal umbilical cord, which can be assessed using this technique (Fig. 18) By the eight week, an embryo's length is between 10 and 16 mm, and the CRL is easily measured. The visualization rate of the fetal aorta and umbilical artery is higher. Blood flow in the fetal heart and aorta as well as in the umbilical artery and intracranial is clearly visualized. At this stage of pregnancy 3D power Doppler imaging allows visualization of the entire fetal circulation.

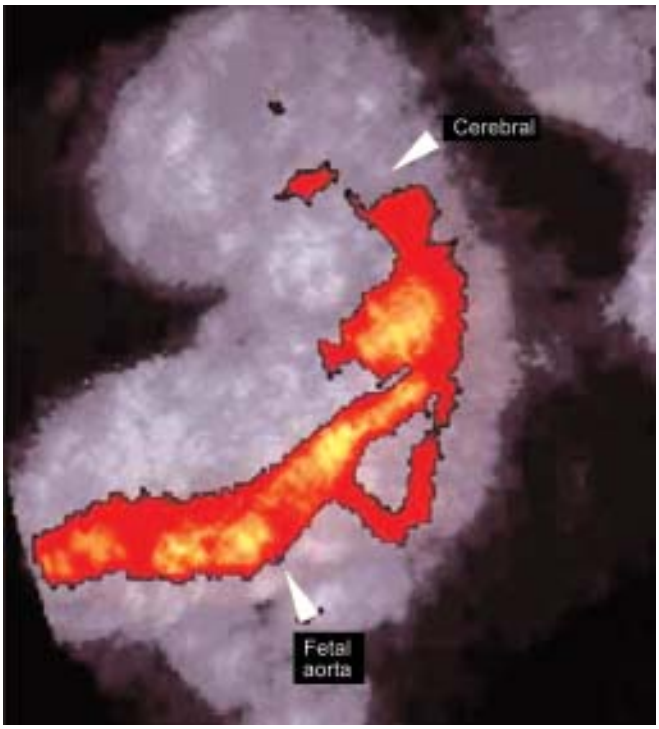

Fig. 18: 3D power Doppler visualized the fetal aorta and umbilical artery. Developing intestine is being herniated into the proximal umbilical cord, which can be assessed using this technique

The 9th-10th Weeks

Characteristic Embryological Findings

The head is more rounded and constitutes almost half of the embryo (Figs 19A and B). The hands and feet approach each other. The upper limbs develop faster than the lower limbs, and toward the end of the 9th week, the fingers are almost entirely formed. The intestines are in the umbilical cord (physiological midgut herniation).

3D Ultrasound Findings

Merz and co-workers[43] were able to provide striking images of the fetal face at this gestational age. They reported cases in which transvaginal 3D ultrasound produced remarkably well-defined facial images as early as 9 weeks gestation. Sometimes even the external ear can be depicted using 3D surface imaging. Herniation of the mid-gut is still present as it is a consequence of the rapid growth of the bowel and liver before closure of the abdominal wall. Although this is a physiologic phenomenon, it does not appear in each fetus. Possibly, we cannot, visualize it, or else its size may vary. At 10 weeks, the bowel undergoes two turns of 180 degrees, returning to its original position, at the same time that closure and development of the abdominal

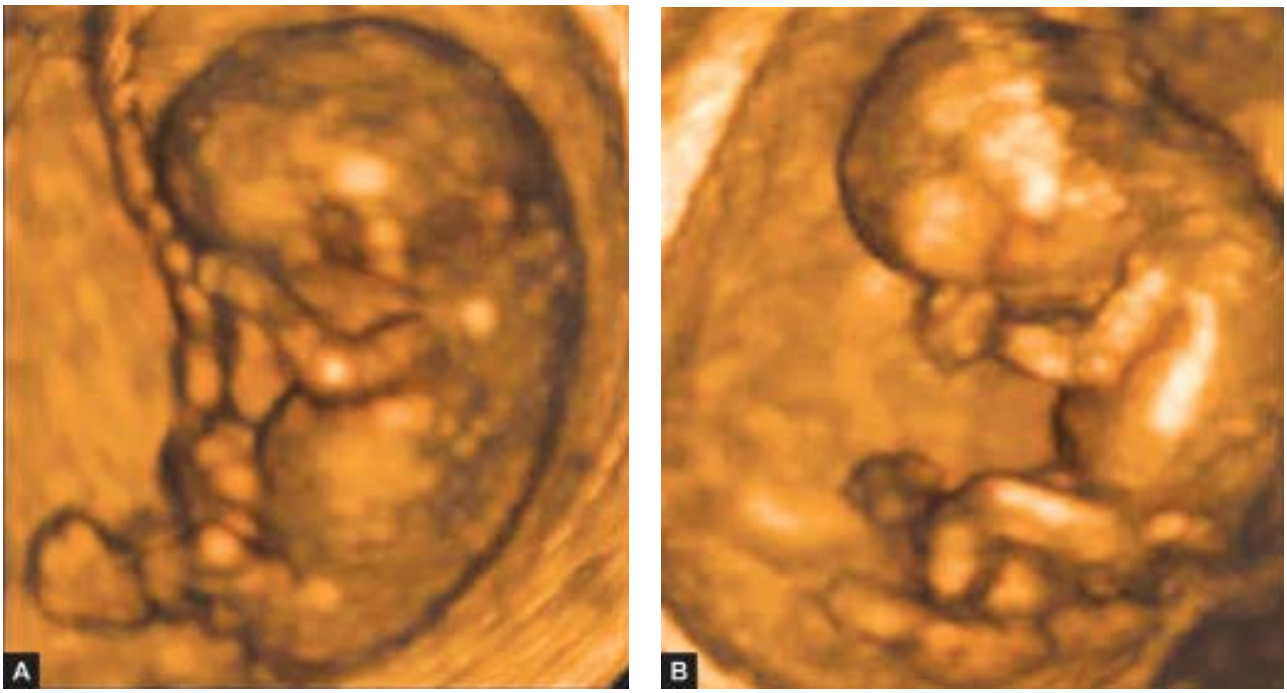

Figs 19A and B: 3D image at 9 weeks (A) and 10 weeks of pregnancy (B). The head is more rounded and constitutes almost half of the embryo. The hands and feet approach each other. The upper limbs develop faster than the lower limbs, and toward the end the fingers are almost entirely formed

wall end. Cerebral hemispheres continue to develop during the 9th and 10th weeks of pregnancy. Visible are lateral ventricles containing hyperechoic choroid plexuses. The head is clearly divided from the body by the neck. External ear is sometimes depicted in the 3D surface image. Herniation of the midgut is present. Dorsal column, the early spine, can be examined in its whole length. The arms with elbow and legs with knees are clearly visible. Feet can be seen approaching the midline.

The size of the lateral ventricles increases rapidly. While the third ventricle is still relatively wide at the beginning of this week, its antero-medial part narrows due to the growth of the thalami. In the fetuses of 25 mm CRL and more, there is a clear gap between the rhombencephalic and the mesencephalic cavity due to the growing cerebellum. The isthmus rhombencephaly is narrow and in most cases, it is not visible in its complete length. The cavity of the diencephalon decreases in the larger fetuses (CRL = 25 mm), and becomes narrow especially at its upper anterior part. The spine is still characterized by two echogenic parallel lines.

3D Power Doppler Findings

Fetal structures are now clearly discernible and they are represented by distinct parts of the fetal body-head, trunk and limbs. The head measures two-thirds of the entire body and becomes a distinct anatomical structure (Fig. 20). The common and internal carotid arteries may be visualized at the end of the eighth gestational week and the beginning of the ninth week. A cerebral circulation (Circle of Willis and its major branches)

Fig. 20: 3D power Doppler image showed the cerebral circulation (Circle of Willis and its major branches) in the form of discrete pulsations of the intracerebral part of the internal carotid artery

can be documented at eight weeks in the form of discrete pulsations of the intracerebral part of the internal carotid artery. From the ninth gestational week, arterial pulsations can be detected on transverse section, lateral to the mesencephalon and cephalic flexure.

The 11th Week

Characteristic Embryological Findings

The mid-gut herniation disappears and fetal kidneys produce urine that is excreted into the amniotic fluid.

3D Ultrasound Findings

During the 11th week of pregnancy development of the head and neck continues. Facial details such as nose, orbits, maxilla and mandibles are often visible (Figs 21A and B). Herniated mid-gut returns into the abdominal cavity. Its persistence after 11th week of gestation is presumptive of an omphalocele. Planar mode enables detailed analysis of the embryonic body with visualization of the stomach and urinary bladder. Kidneys are often visible. Arms and legs continue with development. Hata and co-workers[27] conducted a study on visualization of fetal limbs by 2D and 3D sonography. The ability to visualize fetal hands/fingers and feet/toes was better with 3D than with 2D ultrasonography in the late first trimester (detection rates were 65% and 41% by 3D ultrasonography for hands and feet, respectively and 41% and 12%, by 2D ultrasonography). Long bones can be visualized as hyperechoic elongated structures inside upper and lower extremities. Detailed 3D analysis of the fetal spine, chest and limbs is obtainable by using the transparent, X-ray-like-mode (Figs 21A and B). With the use of the transparency X-ray system, starting at 13 weeks, the medullar channel, each vertebra and rib can be visualized and even the intervertebral disks can be measured. This opens unexpected possibilities for early diagnosis of skeletal malformations.

The 12th Week

Characteristic Embryological Findings

Fetal sex is clearly distinguishable by 12 weeks. The neck is well defined, the face is broad and the eyes are widely separated. By the end of the 12th week, erythropoiesis decreases in the liver and begins in the spleen. The decidua capsularis adheres to the decidua parietalis.

3D Ultrasound Findings

Visualization by 3D ultrasound in 12th week of gestation enables more detailed analysis of fetal anatomy, especially limbs (Fig. 22). It is possible to count fingers and toes. Growing cerebellum is clearly visible. Lateral ventricles dominate the brain.[44]

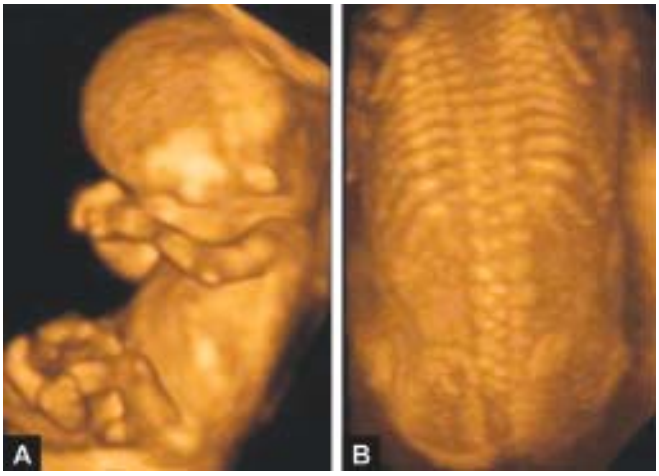

Figs 21A and B: 3D image during the 11th week of pregnancy showing development of the head and neck. Facial details such as nose, orbits, maxilla and mandibles are often visible (A). Detailed 3D analysis of the fetal spine, chest and limbs is obtainable by using the transparent, X-ray-like-mode (B)

Fig. 22: Visualization by 3D ultrasound in 12th week of gestation enables more detailed analysis of fetal anatomy, especially limbs

3D Power Doppler Findings at 11th and 12th Weeks of Gestation

With the use of the 3D power Doppler, it is possible to depict major branches of the aorta: common iliac and renal arteries.

Fig. 23: By using 3D power Doppler technique, it is possible to depict major branches of the aorta: common iliac and renal arteries. Circle of Willis and its branches are easily visible

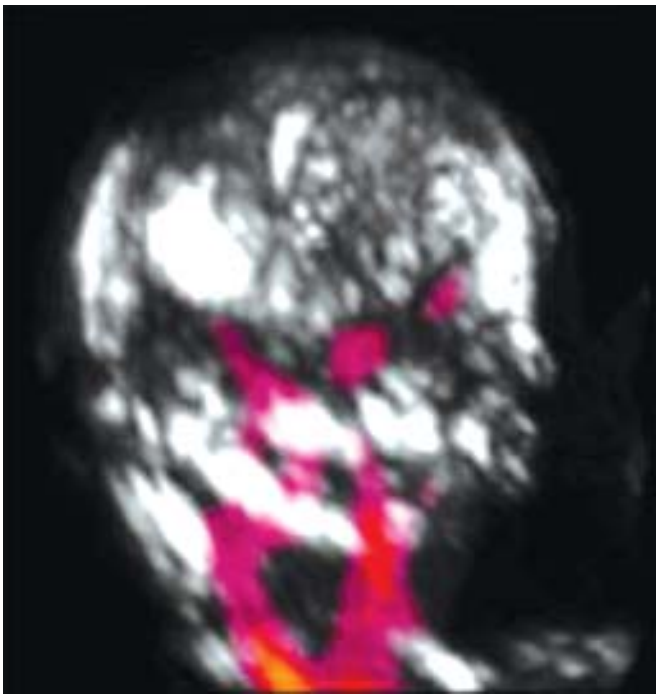

Fig. 24: 3D power Doppler image demonstrated the pulsations of the middle cerebral artery as a separate vessel. However, until the end of the tenth gestational week the ultrasonically detected vascular network should be called intracranial circulation

Circle of Willis and its branches are easily visible (Fig. 23). From this week a more detailed anatomical survey can be obtained, including the cerebral and cardiovascular systems and the digestive and urinary tracts. At this stage, the pulsations of the middle cerebral artery can be easily discerned as a separate vessel. However, until the end of the tenth gestational week the ultrasonically detected vascular network should be called intracranial circulation (Fig. 24). Until the end of the first trimester, the absence of end-diastolic blood flow in fetal and placental components of the circulation is a normal physiological finding.

YALK SAC

3D ultrasound imaging may give additional data to functional Doppler studies for research in developmental anatomy and embryology. This method allows a detailed morphologic and volumetric analysis of extraembryonal static structures. Conventional methods for measuring volumes of fluid-filled spaces include modeling of shapes (e.g. using an ellipsoidal approximation).

Using 3D planar mode, the position of the yolk-sac wall is accurately spatially assessed. Measurement of the volume, rather than estimation from a simple geometric model, increases the accuracy of the measurement. Growth and appearance of the yolk sac have been correlated with the outcome of the pregnancy.[45] Kupesic and Kurjak[46] measured gestational sac volume (Fig. 25) and yolk sac volume and vascularity in pregnancy between 5 and 12 weeks of gestation (Fig. 26). Regression analysis revealed exponential growth of the gestational volume throughout the first trimester of pregnancy.

With the formation of the extraembryonic celomic cavity at the end of the 4th week, the primary yolk sac is replaced with newly-formed secondary yolk sac. During organogenesis and before the placental circulation is established, the yolk sac is the primary source of exchange between the mother and the embryo. It has nutritive, metabolic, endocrine, immunological, excretory and hematopoietic functions. At the beginning of the 5th week, it becomes visible as the first structure inside the chorionic cavity. At this time, a circular, well-defined, echo free area measures 3 to 4 mm in diameter,[47] while the gestational sac measures about 8 to 10 mm. The yolk sac grows slowly until it reaches a maximum diameter of approximately 5 to 6 mm at 10 weeks. It's stalk can be followed from its origin all the way to the embryonic abdomen. As the gestational sac grows and the amniotic cavity expands, the yolk sac as an

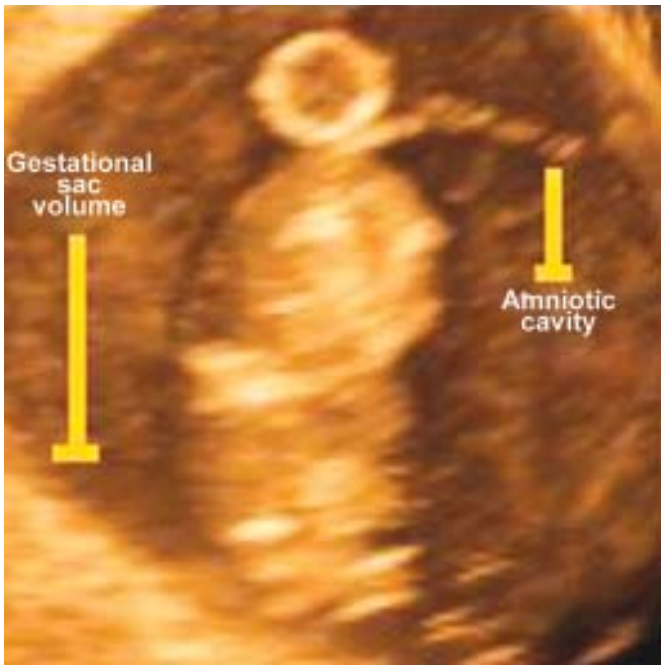

Fig. 25: 3D embryonic structure demonstrated gestational sac and amniotic cavity. Growth and appearance of the yolk sac have been correlated with the outcome of the pregnancy. Regression analysis displayed exponential growth of the gestational volume during the first trimester of pregnancy

extraembryonic structure is gradually separated from the embryo. Different theories exist about the destiny of the yolk sac. Until recently, it was assumed that it gets caught and compressed between amnion and chorion and then ultimately disappears by the end of the 11th week.

Recent studies emphasized that instead of getting compressed the yolk sac degenerates first and then consequently disappears. The ultrasound appearance of the yolk sac (Figs 27A to C) has already been proposed as a prognostic parameter for the outcome of pregnancy. Kurjak and co-workers[48] established some criteria for distinguishing between normal and abnormal yolk sac appearance. In their experience, yolk sac should always be visible before the viable embryo; it measures 4.0 to 5.0 mm in diameter until 7 to 8 weeks of gestation and reaches 6.0 to 6.5 mm by the end of the 9th week. It is evident that sonographic detection of abnormal yolk sac morphology may predict abnormal fetal outcome. Absence of yolk sac, its abnormal size, echogenicity, shape and number are predictive indicators of early pregnancy failure. All these parameters should be defined and assessed prior to 10 gestational weeks. Abnormal yolk sac size may be the first sonographic indicator of associated failure. Primarily, the presence of an embryo without the visible yolk sac before the 10th gestational week is mostly an abnormal finding.

According to some authors, the inner diameter of the yolk sac is always less than 5.6 mm in a normal pregnancy before

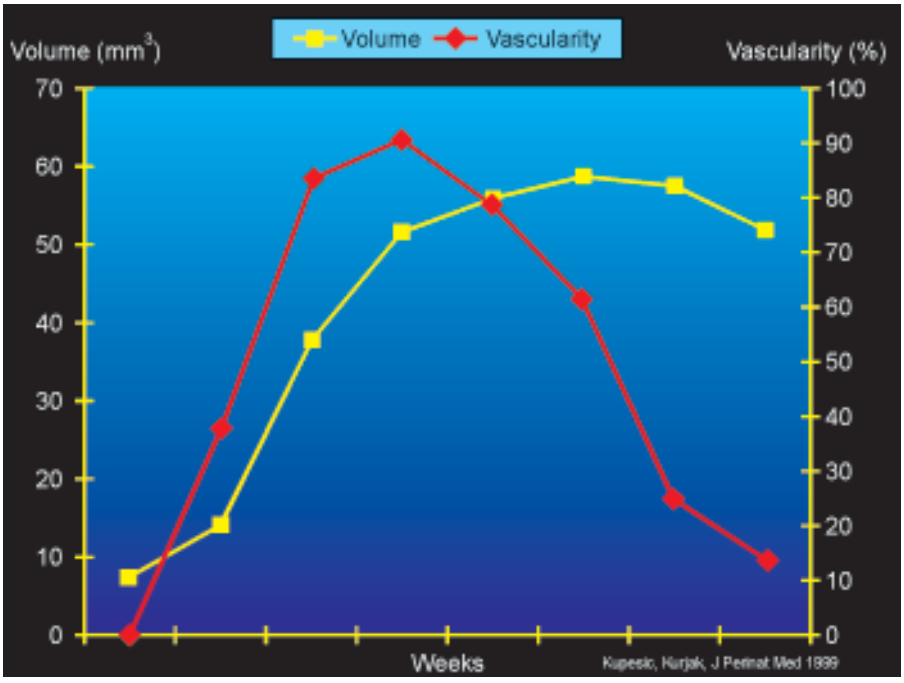

Fig. 26: Vascularity in pregnancy between 5 and 12 weeks of gestation . Regression analysis revealed exponential growth of the gestational sac volume throughout the first trimester of pregnancy

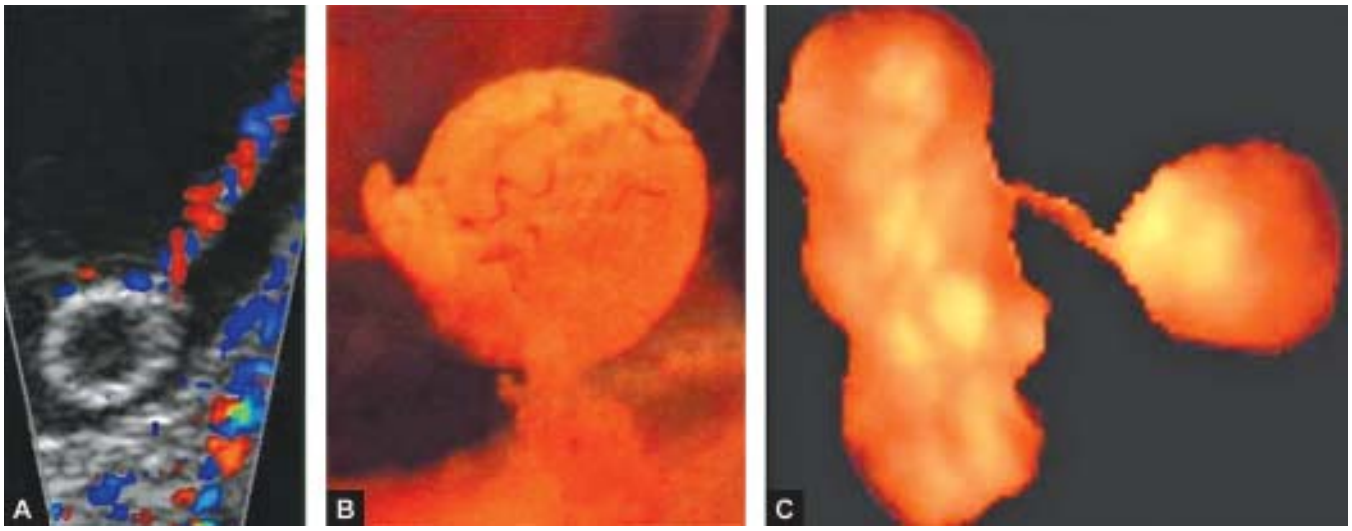

Figs 27A to C: The yolk sac is the primary source of exchange between the mother and the embryo. It has nutritive, metabolic, endocrine, immunological, excretory and hematopoietic functions. (A) At the beginning of the 5th week, using 2D ultrasound it becomes visible as the first structure inside the chorionic cavity. (B) Vizualisation of yolk sac vascularization with fetoscopy. (C) Vizualisation of yolk sac using 3D technique

the 10th week of gestational age. Lyons[49] established that for a mean gestational sac diameter of less than 10 mm, the yolk sac diameter should be less than 4 mm. In 15 patients who had abnormally large sacs, six had no embryo, five aborted spontaneously and only one conceptus survived. Out of nine others with embryo and large yolk sac, eight patients aborted and in one patient trisomy 21 was detected at the 24th gestational week. The yolk sac can be too small, and this is accepted as a marker of poor pregnancy outcome. Green and Hobbins[50] reported a group of patients distributed between 8 and 12 weeks' gestational age, with a yolk sac diameter less than 2 mm associated with an adverse outcome.

It is unknown whether abnormalities of the yolk sac are related primarily to the yolk sac or secondary to the embryonic maldevelopment. According to the present data it seems that the yolk sac plays an important role in materno-fetal transportation in early pregnancy. Changes in size and shape could indicate or reflect the significant dysfunction of this system, and therefore could influence early embryonic development. Currently, major benefits of the sonographic evaluation of the yolk sac are:

1. Differentiation of potentially viable and non-viable gestations,
2. Confirmation of the presence of an intrauterine pregnancy against a decidual cast, and
3. Indication of a possible fetal abnormality.

Recently, Kupesic and associates[51] performed a transvaginal color Doppler study of yolk sac vascularization and volume estimation by 3D ultrasound. They examined 150 patients whose gestational age ranged from 6 to 10 weeks from the last menstrual period during normal uncomplicated pregnancy. Transvaginal 3D and power Doppler examination was performed before the termination of pregnancy for psychosocial reasons. The highest visualization rates for yolk sac vessels were in the 7th and 8th weeks of gestation, reaching value of 90.71%. A characteristic waveform profile included low velocity (5.8 ± 1.7 cm/s), and the absence of diastolic flow was found in all the examined yolk sacs. The pulsatility index showed a mean value of 3.24 ± 0.94 without significant changes between subgroups. The authors found a positive correlation between gestational age and volumes of the yolk sac until 10 weeks of gestation. At the end of the first trimester, yolk sac volume remained constant, while gestational sac volume continued to grow. 3D ultrasound may significantly contribute to *in vivo* observation of the yolk sac's "honeycomb" surface pattern (Fig. 28).

Increased echogenicity of the yolk sac walls were reported as a sign of dystrophic changes that occur in a non-viable cellular material indicating early pregnancy loss.[52] Automatic volume calculation will allow us to estimate precise relationship between the yolk sac and gestational sac volumes, as well as to obtain the correlation between yolk sac volume and CRL measurements. Kupesic and co-workers[53] measured gestational sac volume and yolk sac volume and vascularity in eighty women with uncomplicated pregnancy between 5 and 12 weeks of gestation. Regression analysis revealed an exponential growth of the gestational sac volume throughout the first trimester of pregnancy. Gestational sac volume measurements can be used for estimation of the gestational age in early pregnancy. Abnormal gestational sac volume measurement could potentially be used as a prognostic marker for pregnancy outcome. The yolk sac volume was found to increase from 5 to

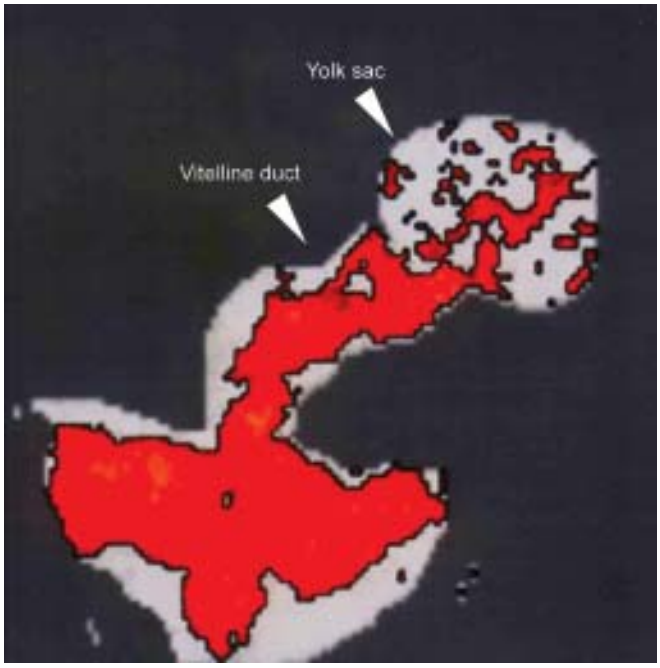

Fig. 28: 3D color Doppler study of yolk sac vascularization demonstrated the yolk sac's "honeycomb" surface pattern. 3D ultrasound and power Doppler will allow us to study turgescent blood vessels withstanding from the surface of the yolk sac

10 weeks of gestation. However, when the yolk sac reaches its maximum volume at around 10 weeks it has already started to degenerate, which can be indirectly proved by a significant reduction in visualization rates of the yolk sac vascularity.

As suggested earlier, the disappearance of the yolk sac in normal pregnancies is probably the result of yolk sac-degeneration rather than of a mechanical compression of the expanding amniotic cavity. These events suggest that the evaluation of the biological function of the yolk sac by measuring the diameter and/or the volume is limited. Therefore, a combination of functional and volumetric studies is necessary to identify some of the more important moments during early pregnancy.

Kurjak et al[48] reported vascularization of the yolk sac in normal pregnancies between 6 and 10 weeks of gestation. Pulsed Doppler signals characterized by low velocity and high pulsatility, were obtained in 85.71% of the yolk sacs during 7th and 8th gestational weeks. Although the reports on yolk sac and vitelline circulation are very exciting, it should be noted that such studies are not ethically feasible in ongoing human pregnancies since the secondary yolk sac is a source of primary germ cells and blood stem cells.[54]

3D ultrasound and power Doppler will allow us to study turgescent blood vessels withstanding from the surface of the yolk sac (Fig. 28). The same technique can be used to study the evolution from the embryo-vitelline towards embryo-placental circulation. Since yolk sac and vitelline blood vessels are prerequisites for the oxygen transfer, absorptive and transfer processes during the first trimester, alterations in this early circulatory system may have some prognostic value for predicting pregnancy outcome.

3D ULTRASOUND IN MULTIPLE PREGNANCY

3D surface rendering may be greatly facilitated determination of chorionicity and amnionicity during the end of first trimester (Figs 29A and B). All of the reliable criteria can be used. These comprise: determining the total number of placentas, determining whether each embryo is within its own amniotic sac, drawing the appearance of the separating membrane, and examining the presence of a triangular projection of placental tissue beyond the chorionic surfaces (Fig. 30).

It is possible to establish a variety of anomalies involving one of a twin pair by high-resolution 3D sonography. It enables the early and precise detection of abnormal multiple pregnancy. Most common anomaly is the early spontaneous demise of one of the fetuses, vanishing twin (Fig. 31). The characteristics of faulty formations affecting twins can be classified into those remarkable to twins, particularly monochorionic twins, like conjoined twins (Fig. 32), and those malformations not unique to twins, such as neural tube defects and congenital heart defects. The most common type of conjoined twins arise from a postimplantation separation of the zygote between the 13th and 16th day following conception is thoracoomphalopagus (28%).[55] Recently, Meizner et al[56] presented on the prenatal diagnosis of thoracoomphalopagus conjoined twins at 9 weeks' gestation. There is still challenge area in early prenatal diagnosis of conjoined twins, especially in choosing accurate treatment options for both parents and the infants.

3D ULTRASOUND AS A TOOL FOR MEASUREMENT OF THE NUCHAL TRANSLUCENCY

The decade of the 1990s has announced in the prospect of first trimester ultrasound screening for fetal chromosomal abnormalities. The technique of measuring nuchal translucency, which gave rise to the remarkably higher detection rate of chromosomal abnormalities, still has to overcome some technical difficulties. The unsuccessful nuchal translucency (NT) measurements were reported in many studies.[57,58] It seems that establishment of the training regimen for NT measurement as reported by Monni et al[59] and Braithwaite et al[60] may overcome some of these methodological problems. Kurjak and co-workers[61] demonstrated that 3D transvaginal ultrasound (Fig. 33) enables the depiction of the successful mid-sagittal section of the fetus, allowing precise NT measurements. This is possible due to the ability of 3D ultrasound to reorient the fetal position using multiplanar imaging. Better intra-observer reproducibility

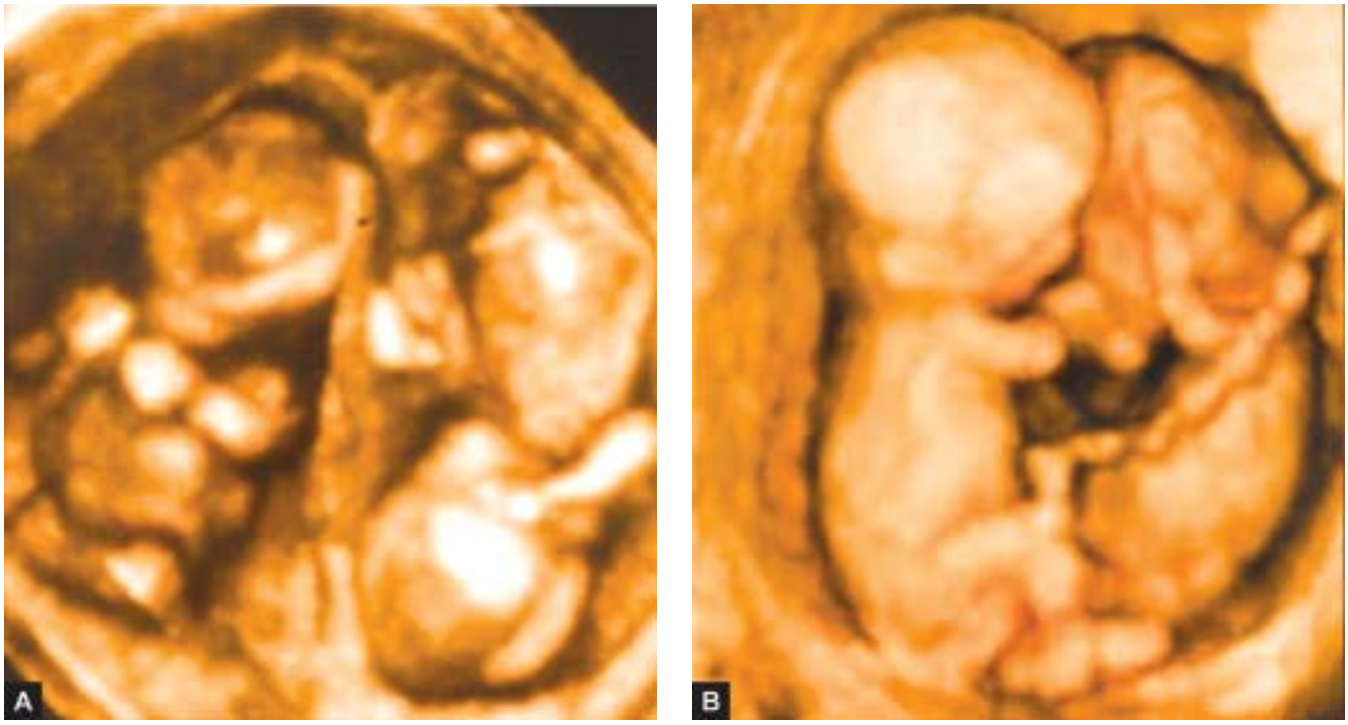

Figs 29A and B: (A) Dichorionic/diamniotic twins at 11 weeks' gestation. (B) Dividing membrane is visualized by 3D surface-mode reconstruction Monochorionic/monoamniotic twins at 11 weeks' gestation

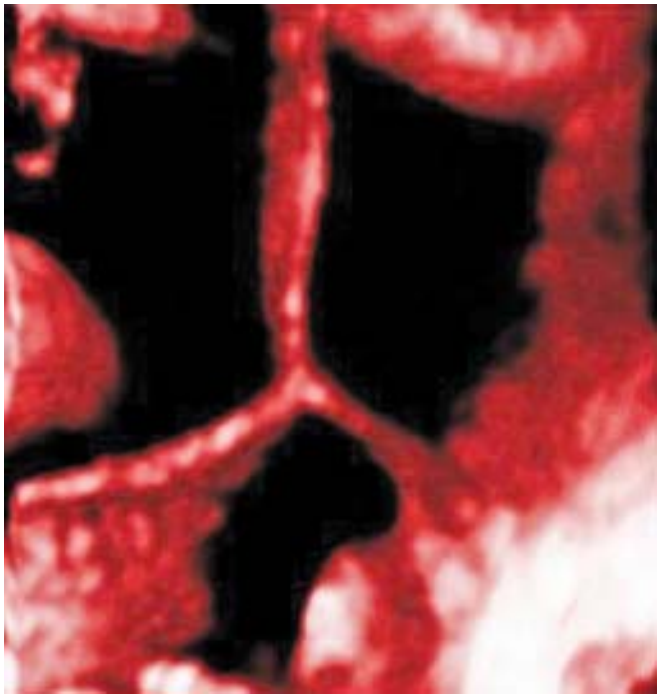

Fig. 30: 3D ultrasound determination of the chorionicity in the late second trimester. "Mercedes" sign represents the junction of fetal membranes

Fig. 31: The early spontaneous demise of one of the fetuses, vanishing twin. Using 3D ultrasound, it is possible to diagnose a variety of anomalies involving one of a twin pair

was obtained for 3D than for 2D ultrasound. 3D transvaginal ultrasound improves accuracy of nuchal translucency measurement allowing appropriate mid-sagittal section of the fetus and clear distinction of the nuchal region from the amniotic membrane.

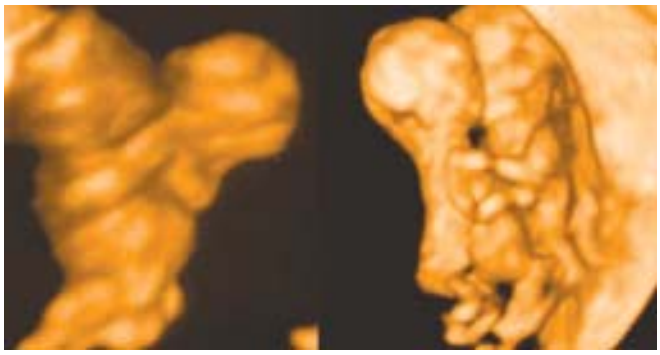

Fig. 32: 3D ultrasound scan of conjoined twins (thoracophagus)

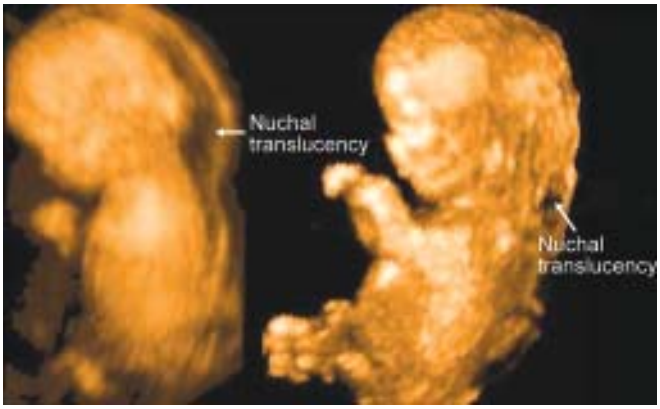

Fig. 33: 3D transvaginal ultrasound enables the depiction of the mid-sagittal section of the fetus, allowing precise NT measurements

3D ULTRASOUND IN EARLY DETECTION OF FETAL ANOMALIES

Anencephaly and Exencephaly (Acrania)

Diagnosis of anencephaly during early pregnancy by ultrasound which is based on the demonstration of absent cranial vault and cerebral hemisphere has been possible for more than 25 years with incidence about 1:1000 births. Diagnosis is established when no bones can be imaging above the orbits, regardless of the quantity of neural soft tissue.[65] Due to many resemblances, it was assumed that exencephaly is a forerunner or a different form of anencephaly.[62-64] The existing record of anencephaly begins with failure of closure of the cephalic end of the neural tube. As a consequence, it implies the absence of the telencephalon, mesencephalon, and failure growth of the cranial vault, comprising the frontal, parietal and occipital bones. A certain amount of brain tissue or angiomatous stroma may develop in several circumstances.[65] It is believed that the primary event is the lack of development of the neuro-cranium.[63,64] As the consequnces, this follows in subsequent degeneration and missing of the brain tissue that is left uncovered to the amniotic fluid.

3D sonography is a very powerful tool for anomaly detection throughout the first trimester. Multiplanar imaging makes possible detailed examination of fetal shape and anatomical structure. Surface mode rendering describes the morphology with sculpture-like appearance, leaving certainly in diagnosis. The lack of cranial development can be discovered exactly. Surface or maximum rendering depicts the abnormal form of the cranium and the complete absence of the development of calvarian bones (Fig. 34).

Encephalocoele

The encephalocoele is caused by lack of ossification of the rostral part of the neural tube. Any part could be affected by imperfection of the ossification and closure of the neural tube. Mostly, the fault is situated posteriorly and in the midline, forming herniation of the meninges and the brain tissue. In the

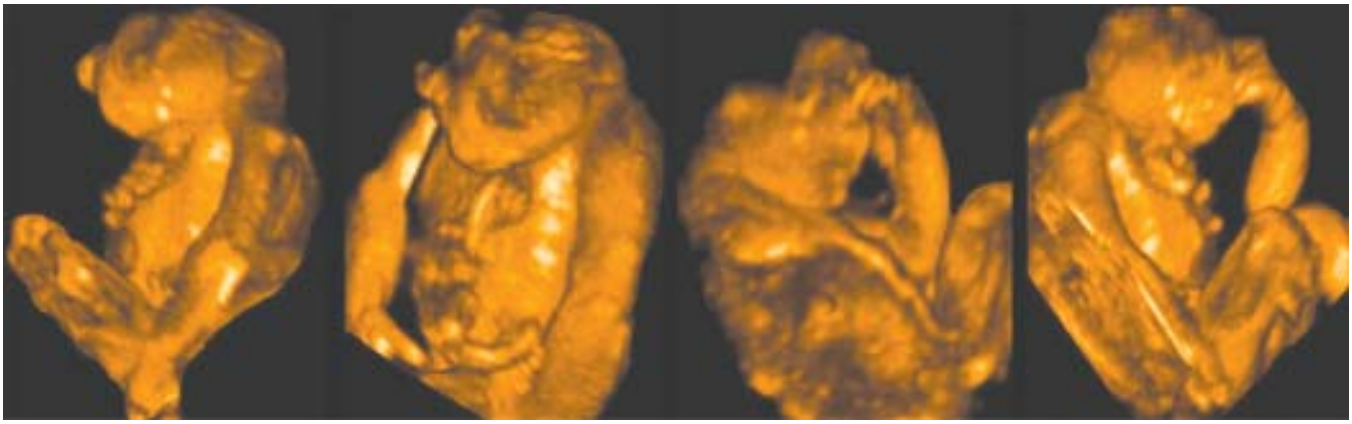

Fig. 34: 3D images of anencephaly. The lack of cranial development can be detected precisely. Surface/maximum rendering depicts the anomalous shape of the cranium and the complete absence of the development of calvarian bones

Fig. 35: 3D sonography can precisely depict the abnormal outline of the head in the case of an encephalocoele. Diagnosis was made upon the finding of bulging meningeal and brain tissue through the defect of the bone

literature, we can find the diagnosis of an encephalocoele at the end of the first trimester.[62] Diagnosis was built on the inquiring of bulging meningeal and brain tissue among the defect of the bone. 3D sonography can exactly describe the anomalous contour of the head in the case of an encephalocoele (Fig. 35). Both multiplanar imaging and surface rendering can be used for this work.

Intracranial Malformations

Hydrocephaly

Hydrocephaly is described by an abnormal collection of the cerebrospinal fluid in the ventricular system of the brain. The blockage can be located at different regions. The most common place is the obstruction of the aqueduct of Sylvius causing accumulation of the cerebrospinal fluid in the lateral and the third ventricles. This results in enlargement of the ventricles because of the growth pressure of the fluid. The enlargement process of the ventricles is progressing by degrees. In this way, it was considered that diagnosis of hydrocephaly was not possible before mid-pregnancy.[66] Diagnosis was established if an irregular hemisphere width to lateral ventricle width was found (Figs 36A and B). Development of 3D ultrasound devices enabled diagnosis of hydrocephaly in early pregnancy.[67,68] Visualization and measurement of the choroid plexus is possible from the 11th week of gestation. In a normal brain choroid plexus fills the atrium and the body of the lateral ventricle. When

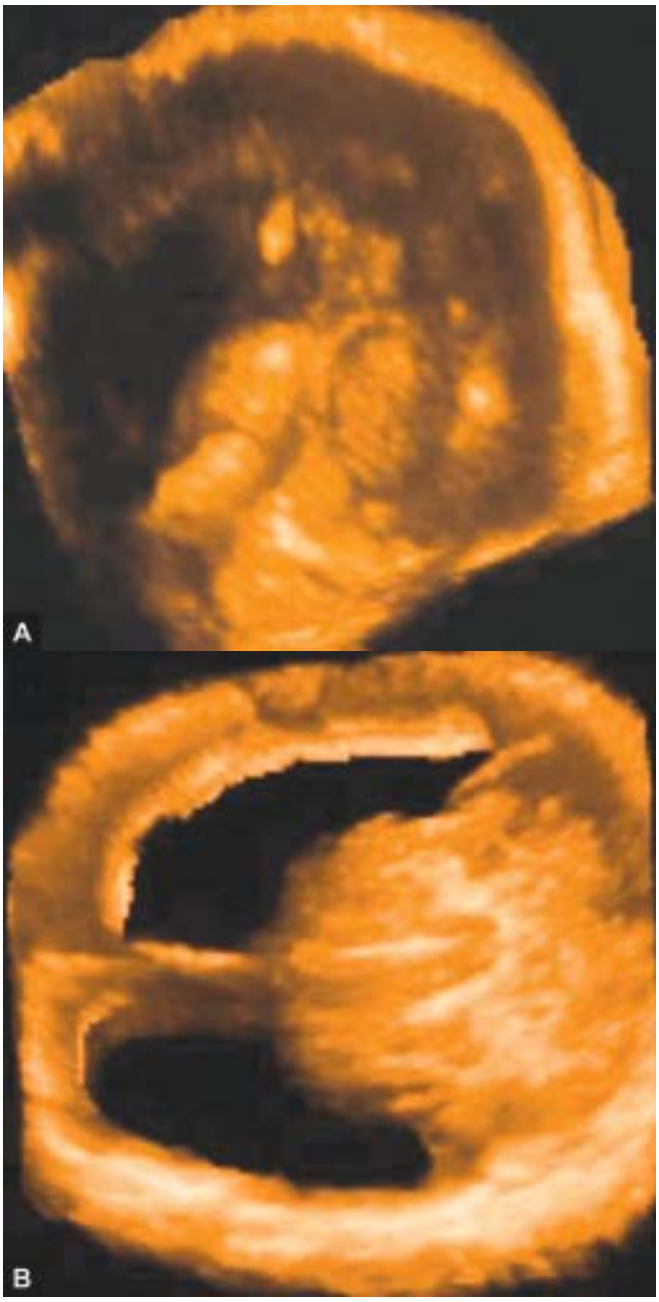

Figs 36A and B: 3D reconstruction of the abnormality of the posterior fossa is clearly demonstrated (A). Multiplanar 3D analysis helpful for fast selection of the adequate section of the abnormal lateral ventricle in hydrocephaly (B)

pressure of the cerebrospinal fluid rises, the dilatation of the lateral ventricles gives a particular appearance to the choroid plexus.[69]

Holoprosencephaly

Holoprosencephaly arises from absent or incomplete separation of the prosencephalon in two cerebral hemispheres and lateral

ventricles. It is classified into alobar, semilobar and lobar types.[70]

The most severe is alobar holoprosencephaly that occurs after a total ceasing of prosencephalon cleavage. This produces formation of a monoventricular cavity with thalamus and basal ganglia fused in the midline, while the midbrain, brainstem and cerebellum are structurally normal. Alobar holoprosencephaly is frequently connected with serious facial malformations for example cleft lip and palate, severe hypotelorism and cyclopia, arrhinia with proboscis and also can be found in some aneuploidies, usually trisomy 13 and trisomy 18. A frontal monoventricle is present in the semilobar holoprosencephaly and there is posterior partial formation of the occipital lobes. In the lobar holoprosencephaly the hemispheres may be fused and the lateral ventricles may extensively communicate because of the absence of the septum pellucidum. Due to severe interruption of the normal intracranial anatomy ultrasound diagnosis of holoprosencephaly can be done at the end of the first trimester.[71,72] The lack of normally grown telencephalon including hyperechoic choroid plexi, frontally positioned monoventricle, and facial anomaly (severe hypotelorism) are characteristics that should support sufficient diagnosis (Fig. 37). 3D sonography enables careful and precise analysis of anatomical features in very early pregnancy, making the diagnostic process accurate and fast.

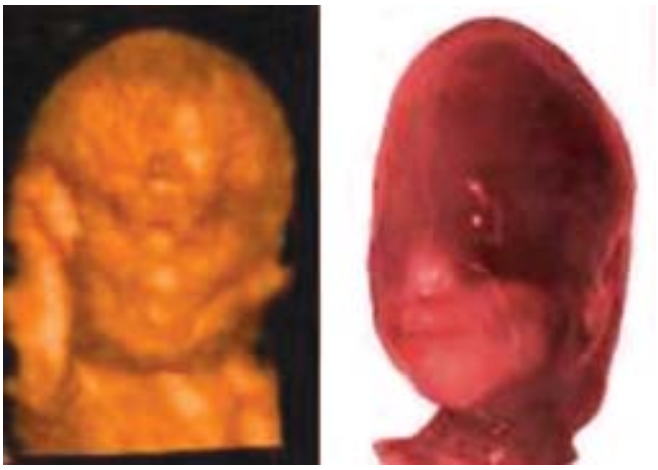

Fig. 37: 3D sonography image of holoprosencephaly at 12 weeks of gestation (Trisomy 13). Compare the 3D finding of hypotelorism with the postmortem fetus. 3D sonography enables analysis of anatomical features in early pregnancy, making the diagnostic process accurate and fast

DYNAMIC REAL TIME 3D ULTRASOUND (4D TECHNIQUE) AS A TOOL FOR ASSESSMENT OF FETAL BEHAVIOR IN EARLY PREGNANCY

3D sonography has become the new standard in prenatal diagnosis. This technique enables detailed examination of the fetal anatomy and higher quality depiction of some anomalies. Until recently, the main drawback of 3D sonography was its inability to present a real-time motional image. Furthermore, motoric activity of the fetus yielded with significant artifacts in the image, making it inadequate for diagnostic purposes. 3D depiction is technologically based on high velocity processing of the data. Development of the computer processors was the essential prerogative for 3D ultrasound devices. The latest development of calculating units enables 3D reconstruction at a frame rate of up to 20 images per second. In the human eye this frame rate produces quite smooth dynamic real-time 3D images, also known as 4D image.[73]

The first trimester of pregnancy is a period of early human development of incomparable intensity. Before the 'ultrasound era' investigation of this field was reserved for post mortem embryological analysis. However, transvaginal real time B-mode, color Doppler, and, in the last few years, different forms of 3D sonography have enabled non-invasive and safe investigation *in vivo*. Due to the size of the pregnant uterus and relatively large amount of fluid surrounding the embryo, the first trimester is very suitable for 4D sonography. We already investigated embryonic or fetal movements and several movements were classified as following (Fig. 38):

- Gross body movements consisted of changing the position of the head towards the body
- Limb movements consisted of changes in position of extremities towards the body without extension or flexion in elbow or knee
- Complex limb movements consisted of changes in position of the limb segments towards each other, such as extension or flexion in elbow or knee.

According to CRL the pregnant women were divided into four groups:

- Group 1: CRL < 9 mm (less than 7 weeks of gestation)
- Group 2: CRL > 9 mm and < 15 mm (between 7 and 8 weeks)
- Group 3: CRL > 16 mm and < 30 mm (between 8 and 10 weeks)
- Group 4: CRL > 31 mm and < 50 mm (between 10 and 12 weeks).

Matters of interest were the gestational age at which each of these three kinds of movements appeared, and their visualization with advanced technology. A total of 98 pregnant women were analyzed. In the first group no movements were found. In the other groups, the incidence of each type of embryonic or fetal movements is presented in Table 1.

At the seventh week 38% embryos had spontaneous gross body movements. At this gestational age we found no limb movements. In 42% of fetuses from the third group spontaneous gross body movements were presented. Furthermore, in 26%

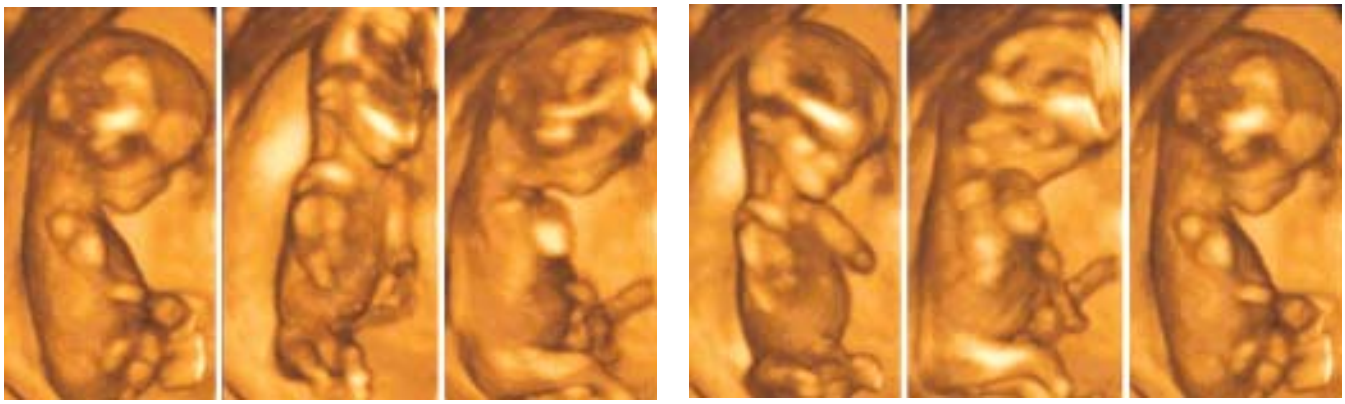

Fig. 38: 4D ultrasound sequence of the fetus at 12 weeks of gestation showing general movements. The complex movements of the limb, trunk and head are clearly visible and cause a shift in fetal position. In the first sequence, the right hand is flexed in elbow joint. In the next sequence, the fetus dropped the hand and began to deflect in elbow joint. In the last sequence, further elevation of hand is seen

Table 1: The incidence of spontaneous embryonic/fetal movement according to gestational age

Gestational age (weeks)	*CRL (mm)*	*No movements*	*Gross body movements*	*Limb movements*	*Complex limb movements*
7-8	0-15	31	12	0	0
9-10	16-30	26	11	7	0
11-12	31-50	19	16	12	8

Source: Adapted from Kurjak A et al (2002)[74]

of fetuses only simple limb movements were visualized at this gestational age. In 84% of fetuses from the fourth group gross body movements and in 63% limb movements were presented. Additionally, in 42% spontaneous complex limb movements were visualized.

The straightforward development of 3D ultrasound has led to the possibility of performing 3D imaging in a real-time mode. This modality has been named 4D sonography. This improvement greatly facilitates the assessment of fetal movements because they can be visualized in three dimensions. Thus it is much easier to assess fetal motoric status than with 2D. For each embryonic structure there is a period between genesis and ultrasonic visualization.[75] As technology advances the period becomes shorter. Limbs begin to move from week seven onwards.[76] Using 2D transvaginal ultrasound technique body movements are visualized between weeks eight and nine, and limb movements are visualized between weeks nine and ten.[77] The embryo body movements, which were absent before seven weeks of gestation, were observed after eight weeks with a sensitivity of 100%, specificity of 92.8%, positive predictive value of 94.3%, and negative predictive value of 100%.[78] With 4D we found gross body movement at seven weeks, and limb movements at weeks eight to nine. New technology enables the visualization of the moving phenomenon a week earlier than 2D transvaginal ultrasound. The use of 4D technology should thus enable the diagnosis of motoric development failure at the end of the first trimester. It also makes possible the evaluation of complex limb movement, the visualization of simultaneous movement of all extremities and the spatial evaluation of movements.

At seven gestational weeks the dominant embryonic feature is the head that is strongly flectioned anteriorily. Upper and lower limb buds are visible on the lateral aspects of the embryo. However, embryonic movements are not frequent and consist mainly of moving the head towards the rest of the body, while fetal limb movements are absent.[74]

At eight to nine weeks the embryo has different body features to be observed. The head is less flectioned and limbs are elongated. Segments of the arms and legs are distinguishable. Embryonic movements can be divided in two main groups: gross body movements that consist of changes of the position of the head towards the body and movements of the extremities: arms and legs are moved vigorously. However no flexion or extension in elbow or knee can be seen.[74]

At ten to twelve weeks of gestation complex body and limb movements can be seen. At this gestational age there was a great resemblance of fetal movements to those in neonates.

Using the advantages of 4D technology a physiologic pattern of embryonic or fetal motor development was made. Any alteration from the pattern should be an indication for further

diagnostic engagement. Development of the limbs is a complex process that consists of tissue differentiation (cartilage, muscle, nerves, blood vessels and tendons). An insult on each tissue in the differentiation process can alter the developmental pattern. An alteration of motor development can be a consequence of delayed or aborted motor development.

Delay in motoric development has been described in diabetic pregnancies.[79] There is a one to two week delay in the first appearance of all movement patterns, which normally emerge during the first twelve weeks of pregnancy. This indicates the possible existence of a specific diabetes-related influence on the functional development of the embryonic and fetal nervous system. Hyperglycemia, for example, may be responsible, as the delay in the emergence of fetal general movements was most profound in women whose periconceptional quality of glucose control was poor.[79] Limb movements are essential to the normal development of joints.[76] Early disturbances in motoric development result in absence of limb movement, joint contracture and multiple joint contracture (arthrogryposis). Spinal muscular atrophy is characterized with multiple arthogryposis.[80]

Four-dimensional (4D) ultrasound technology offers a possibility to predict the development of arthrogryposis in high risk pregnancies on the basis of the evaluation of fetal movements. Etiology of the disease is the progressive degeneration of anterior horn cells in the spinal cord and motor nuclei in brainstein.[74]

We also noticed lateralization of movements. There was a highly significant preference for fetuses to move their right arm more than their left arm. This observation agrees with Hepper's findings.[81] In his study 85% of fetuses exhibited more right arm than left arm movements.

REFERENCES

1. Baba K, Satoh K, Sakamoto S, et al. Development of an ultrasonic system for three-dimensional reconstruction of the fetus. J Perinat Med 1989;17:19.
2. Fredfelt KE, Holm HH, Pedersen JF. Three-dimensional ultrasonic scanning. Acta Radiol Diagn 1984;25:237.
3. Chiba Y, Hayashi K, Yamazaki S, et al. New techniques of ultrasound, thick slicing 3D imaging and the clinical aspects in perinatal field. Ultrasound Obstet Gynecol 1994;4:195.
4. Gregg A, Steiner H, Staudach A, et al. Accuracy of 3D sonographic volume measurements. Am J Obstet Gynecol 1993;168:348.
5. Kossof G, Griffiths KA, Warren PS, et al. Three dimensional volume imaging in obstetrics. Ultrasound Obstet Gynecol 1994;4:196.
6. Kou HC, Chang FM, Wu CH, et al. The primary application of three-dimensional ultrasonography in obstetrics. Am J Obstet Gynecol 1992;166:880.
7. Merz A, Macchiela D, Bahlamann F, et al. Three-dimensional ultrasound for the diagnosis of fetal malformations. Ultrasound Obstet Gynecol 1992;2:137.
8. Pretorius DH, Nelson TR. Three-dimensional ultrasound. Opinion. Ultrasound Obstet Gynecol 1995;5:219.
9. Feichtinger W. Transvaginal three-dimensional imaging. Editorial. Ultrasound Obstet Gynecol 1993;3:375.
10. Baba K, Okai T. Clinical applications of three-dimensional ultrasound in obstetrics. In Baba K, D Jurkovic (Eds): Three-dimensional ultrasound in Obstetrics and Gynecology. New York-London, The Parthenon Publishing Group 1997;29.
11. Miric-Tesanic D, Kurjak A. Trodimenzionalni ultrazvuk u ginekologiji i porodništvu. Ginekol Perinatol 1997;6:43.
12. Merz E, Bahlmann F, Weber G. Volume 3D scanning in the evaluation of fetal malformations: a new dimension in prenatal diagnosis. Ultrasound Obstet Gynecol 1995;4:222.
13. Merz E, Bahlmann F, Weber G, et al. Volume 3D scanning : a new dimension in the evaluation of fetal malformations. Ultrasound Obstet Gynecol 1993;3:131.
14. Kurjak A, Kupešc S. Three-dimensional transvaginal ultrasound improves measurment of nuchal translucency. J Perinat Med 1999;27-91.
15. Bonilla-Musoles F. Three-dimensional visualization of the human embryo: a potential revolution in prenatal diagnosis. Editorial. Ultrasound Obstet Gynecol 1996;7:393.
16. Bonilla-Musoles F, Raga F, Osborne N, Blanes J. The use of three-dimensional (3D) ultrasound for study of normal pathologic morphology of the human embryo and fetus: preliminary report. J Ultrasound Med 1995;14:757.
17. Lee A, Deutinger J, Bernaschek G. Three-dimensional ultrasound: abnormalities of the fetal face in surface and volume rendering mode. Br J Obstet Gynaecol 1995;102:40.
18. Lee A, Deutinger J, Bernaschek G. Voluvision: Three-dimensional ultrasonography of fetal malformations. Am J Obstet Gynecol 1994;170:1312.
19. Lee A, Kratochwil A, Deutinger J, et al. Three-dimensional ultrasound in diagnosing phocomelia. Ultrasound Obstet Gynecol 1995;5:238.
20. Maymon J, Halperin Z, Weinraub A, Herman A, Schneider D. Three-dimensional sonography of conjoined twins at 10 weeks: a case report. Ultrasound Obstet Gynecol 1998;11:292.
21. Pretorius DH, Nelson TR. Three-dimensional ultrasound of fetal surface features. Ultrasound Obstet Gynecol 1992;2:166.
22. Blaas HG, Eik-Nes SH, Berg S, Torp H. *In vivo* three-dimensional ultrasound reconstructions of embryos and early fetuses. Lancet 1998;352:1182.
24. Benoit B, Hafner T, Bekavac I, Kurjak A. Three-dimensional sonoembryology. Ultrasound Rev Obstet Gynecol 2001;1:111.
24. Kurjak A, Zudenigo D, Predanic M, Kupesic S, Funduk-Kurjak B. Transvaginal color Doppler study of fetomaternal circulation in threatened abortion. Fetal Diagn Ther 1994;9:341.
25. Kupesic S, Bekavac I, Bjelos D, Kurjak A. Assessment of Endometrial Receptivity by Transvaginal Color Doppler and Three-dimensional Power Doppler Ultrasonography in Patients Undergoing *In Vitro* Fertilization Procedures. J Ultrasound Med 2001;20:125-34.

26. Itskovitz J, Lindenbaum ES, Brandes JM. Arterial anastomosis in the pregnant human uterus. Obstet Gynecol 1980;1:3-19.
27. Kurjak A, Zudenigo D, Funduk-Kurjak B, Shalan H, Predanic M, Sosic A. Transvaginal color Doppler in the assessment of the uteroplacental circulation in normal early pregnancy. J Perinat Med 1993;21:25-34.
28. Kurjak A, Kupesic S, Predanic M, Salihagic A. Transvaginal color Doppler assessment of the uteroplacental circulation 111 normal and abnormal early pregnancy. Early Human Dev 1992;29(1-3):385-89.
29. Jauniaux E, Jurkovic D, Campbell S. *In vivo* investigations of anatomy and physiology of early human placental circulation. Ultrasound Obstet Gynecol 1991;1:435-45.
30. Jaffe R, Warsof SL. Transvaginal color Doppler imaging in the assessment of uteroplacental blood flow in the normal first trimester pregnancy. Am J Obstet Gynecol 1991;164:781-85.
31. Kurjak A, Kupesic-Urek S, Predanic M, Zudenigo D, Matijevic R, Salihagic A. Transvaginal color Doppler in the study of early pregnancies associated with fibroids. J Matern Fetal Invest 1992;2:81-87.
32. Pijnenborg R, Bland JM, Robertson WB, Brosens I. Uteroplacental arterial changes related to interstitial trophoblast-migration in early human pregnancy. Placenta 1983;4:397-14.
33. Pijnenborg R, Dixon G, Robertson WB, Brosens I. Trophoblastic invasion of human decidua from 8 to 18 weeks of pregnancy. Placenta 1986;1:3-19.
34. Kanayama N. Trophoblast injury: a new etiological and pathological concept of preeclampsia. Croat Med J 2003;44 (2):148-56.
35. Kurjak A, Kupesic S. Doppler proof of the presence of intervillous circulation (Letter). Ultrasound Obstet Gynecol 1996;7:463.
36. Kurjak A, Laurini R, Kupesic S, Kos M, Latin V, Bulic K. A combined Doppler and morphopathological study of intervillous circulation. Book of Abstracts. The Fifth World Congress of Ultrasound in Obstetrics and Gynecology, Kyoto, 25-29 November, 1995. Ultrasound Obstet Gynecol 1995;6(suppl)116.
37. Kurjak A, Predanic M, Kupesic S, Zudenigo D, Matijevic R, Salihagic A. Transvaginal color Doppler in the study of early normal pregnancies and pregnancies associated with uterine fibroids. J Matern Fetal Invest 1992;3: 81.
38. Kurjak A, Kupesic S, Banovic I, Hafner T, Kos M. The study of morphology and circulation of early embryo by three-dimensional ultrasound and power Doppler. J Perinat Med 1999;27:145-57.
39. Kupesic S, Kurjak A, Ivancic-Kosuta M. Volume and vascularity of the volk sac studied by three-dimensional ultrasound and color Doppler. J Perinat Med 1999;27:91-96.
40. Bonilla-Musoles, et al. Dernonstration of Early Pregnancy with Three-Dimensional Ultrasound. In Merz E (Ed): 3D Ultrasound in Obstetrics and Gynecology. Lippincott Williams & Wilkins, Philadelphia, New York, Baltimore 1998;31-37.
41. Blaas HG, Eik-Nes SH, Kiserud T, Berg B, Angelsen B, Olstad B. Three-dimensional imaging of the brain cavities in human embryos. Ultrasound Obstet Gynecol 1995;5:228-32.
42. O'Rahilly R, Mueller F. Ventricular system and choroid plexuses of the human brain during the embryonic period proper. Am J Anat 1990;189:285-302.
43. Merz E, Weber G, Bahlmann F, Miric-Tesanic D. Application of transvaginal and abdominal three-dimensional ultrasound for the detection or exclusion of fetal malformations of the fetal face. Ultrasound Obstet Gynecol 1997;9:2373.
44. Kurjak A, Zodan T, Kupesic S. Three-dimensional sonoembryology of the first trimester. In Clinical application of 3D sonography (Eds): Kurjak A, Kupesic S. The parthenon publishing NY, London, 2000,109-21.
45. Lindsay DJ, EA Lyons, CS Levi, XH Zheng. Endovaginal appearance of the yolk sac in early pregnancy: normal growth and usefulness as a predictor of abnormal pregnancy outcome. Radiology 1988;166:109.
46. Kupesic S, A Kurjak. Volume and vascularity of the yolk sac studied by three-dimensional ultrasound and color Doppler. J Perinat Med 1999;27:97.
47. Lindsay DJ, Lovett IS, Lyons EA, Levi CS, Zheng XH, Holt. SC, Dashefsky SM. Endovaginal appearance of the volk sac in pregnancy: normal growth and usefulness as a predictor of abnormal pregnancy outcome. Radiology 1992;183:115-18.
48. Kurjak A, Kupesic S, Kostovic L. Vascularization of yolk sac and vitelline duct in normal pregnancies studied by transvaginal color Doppler. J Perinat Med 1994;22:443.
49. Lyons EA. Endovaginal sonography of the first trimester of pregnancy. Proceedings of the 3rd Intemational Perinatal and Gynecological Ultrasound Symposium Ottawa, Ontario, 1994;1-25.
50. Green JJ, Hobbins JC. Abdominal ultrasound examination of the first trimester fetus. Am J Obstet Gynecol 1988;159:165-75.
51. Kupesic S, Kurjak A. Volume and vascularity of yolk sac assessed by three-dimensional and power doppler ultrasound; Early Pregnancy 2001;5(1):40-41.
52. Harris RD, Fvincent LM, Askin FB. Yolk sac calcification: A sonographic finding associated with intrauterine embryonic demise in the first trimester. Radiology 1988;166:109.
53. Kupesic S, Kurjak A, Ivancic-Kosuta M. Volume and vascularity of the yolk sac studied by three-dimensional ultrasound and color Doppler. J Perinat Med 1999;27:91-96.
54. Witschi E. Migration of the germ cells of human embryos from the yolk sac to the primitive gonadal folds. Contrib Embryol Carnegie Inst 1948;32:67.
55. Edmonds LD, PM Layde. Conjoined twins in the United States 1970-1977. Teratology 1982;25:301.
56. Meizner I, Levy A, Katz M, Glezerman M. Early ultrasonic diagnosis of conjoined twins. Harefuah 1993;124:741.
57. Roberts LJ, Bewley S, Mackinson AM, Rodeck CH. First trimester nuchal translucency: Problems with screening the general population I. Br J Obstet Gynaecol 1995;102:381.
58. Haddow JE, Palomokie GE. Down's syndrome screening. Lancet 1996;347:1625.
59. Monni G, Zoppi MA, Ibba RM, Floris M. Fetal nuchal translucency test for Down's syndrome. Lancet 1997;350:1631.

60. Braithwaite JM, Economides DL. The assessment of nuchal translucency with transabdominal and transvaginal sonography-success rates, repeatability and level of agreement. Br J Obstet Gynaecol 1995;68:720.
61. Kurjak A, Kupesic S, Ivancic-Kosuta M. Three-dimensional transvaginal ultrasound improves measurement of nuchal translucency. J Perinat Med 1999;27:97-102.
62. Achiron R, Achiron A. Transvaginal fetal neurosonography: the first trimester of pregnancy. In Chervenak FA, A Kurjak, CH Comstock (Eds): Ultrasound and the fetal brain. Parthenon Publishing, London-New York 1995;95.
63. Achiron R, Malinger G, Tadmor O, Diamant Y, Zakut H. Exencephaly and anencephaly: a distinct anomaly or an embryologic precursor: *in utero* study by transvaginal sonography. Israel J Obstet Gynecol 1990;1,60.
64. Goldstein RB, Filly RA, Callen PA. Sonography of anencephaly: pitfalls in early diagnosis. J Clin Ultrasound 1989;17:397.
65. Hudgins RJ, Edwards MSB, Goldstein R, Callen PW, Harrison MW, Filly RA, Golbus MS. Natural history of fetal ventriculomegaly. Pediatrics 1988;82:692.
66. Cardoza JD, Goldstein RB, Filly RA. Exclusion of fetal ventriculomegaly with a single measurement: the width of the lateral ventricular atrium. Radiology 1988;169:711.
67. Bronstein M, Ben-Shlomo I. Choroid plexus dysmorphism detected by transvaginal sonography: The earliest sign of fetal hydrocephalus. J Clin Ultrasound 1991;19: 547.
68. Goldstein RB, LaPidus AS, Filly RA, Cardoza J. Mild lateral cerebral ventricular dilatation *in utero*: clinical significance and prognosis. Radiology 1990;176:237.
69. Cohen M, Jirasek J, Guzman R, Gorlin R, Peterson M. Holoprosencephaly and facial dysmorphia:nosology, etiology, and pathogenesis. Birth Defects 1971;7:125.
70. Edmonds LD, Layde PM. Conjoined twins in the United States 1970-1977. Teratology 1982;25:301.
71. Nelson LH, King M. Early diagnosis of holoprosencephaly. J Ultrasound Med 1992;11:57.
72. Achiron R, Achiron A, Lipitz S, Maschiach S, Goldman B. Holoprosencephaly: alobar. Fetus 1994;4:9.
73. Lee A. Four-dimensional ultrasound in prenatal diagnosis: leading edge in imaging technology. Ultrasound Rev Obstet Gynecol 2001;1:144.
74. Kurjak A, Vecek N, Hafner T, Bozek T, Kurjak BF, Ujevic B. Prenatal diagnosis: what does four-dimensional ultrasound add? J Perinat Med 2002;30:57-62.
75. Kurjak A, Kupesic S, Banovic I, Hafner T, Kos M. The study of morphology and circulation of early embryo by three-dimensional ultrasound and Power Doppler. J Perinat Med 1999;27:145.
76. McLachlan J. Medical embryology. Addison-Wesley 1994.
77. Timor-Tritsch IE, Farine D, Rosen. Close look at early embryonic development with high frequency transvaginal transducer. Am J Obstet Gynecol 1988;159:676.
78. Goldstein I, Zimmer EA, Tamir A, Peretz BA, Paldi E. Evaluation of normal gestational sac growth: appearance of embryonic heartbeat and embryo body movements using the transvaginal technique. Obstet Gynecol 1991;78:729.
79. Mulder EJ, Visser GH. Growth and motor development in fetuses of women with type-1 diabetes. II. Emergence of specific movement patterns. Early Hum Dev 1991;25:107.
80. Lauders H, Meerbach W, Grauel BM. Unusual Complications at birth an a stillborn with spinal muscular atrophy. Zentralbl Allg Pathol 1988;134:567.
81. Hepper PG, McCartney GR, Shannon EA. Lateralised behaviour in first trimester human foetuses. Neuropsychologia 1998;36,531.